GEOMETRIC CHARACTERIZATION OF THE WORKSPACE OF NON-ORTHOGONAL ROTATION AXES

BERTOLD BONGARDT

Abstract. In this article, a novel characterization of the workspace of 3R chains with non-orthogonal, intersecting axes is derived by describing the set of singular orientations as two toroids that separate two-solvable from non-solvable orientations within $SO(3)$. Therefore, the toroids provide the boundary of the workspace of the axes' constellation. The derived characterization generalizes a recent result obtained by Piovan and Bullo. It is based on a specific, novel representation of rotations, called *unit ball representation*, which allows to interpret the workspace characterization with ease. In an appendix, tools for dealing with angles and rotations are introduced and the equivalence of unit quaternion representation and unit ball representation is described.

1. Introduction

A classic problem in mechanics is to decompose an orientation into a sequence of rotations along three intersecting axes. For example, this decomposition is applied if the representation of a rotation as a triplet of *Euler angles* is computed. In this case, the rotation axes are chosen as sequentially perpendicular coordinate axes [14]. For arbitrary axes, the problem is defined as follows.

Problem 1 (Rotation Decomposition)**.** *Given three rotation axes $\hat{\boldsymbol{\omega}}_1$, $\hat{\boldsymbol{\omega}}_2$, $\hat{\boldsymbol{\omega}}_3$, and an orientation $\boldsymbol{R} \in SO(3)$, compute angles ϕ_1, ϕ_2, and ϕ_3 such that*

$$\boldsymbol{R} = \boldsymbol{R}(\phi_1;\hat{\boldsymbol{\omega}}_1) \cdot \boldsymbol{R}(\phi_2;\hat{\boldsymbol{\omega}}_2) \cdot \boldsymbol{R}(\phi_3;\hat{\boldsymbol{\omega}}_3)\,. \tag{1}$$

In this general version, the problem appears as the inverse kinematics problem of spherical 3R chains, for example at special 'wrists' [18] of robot arms. A solution of Problem 1 is described, for example, in [17, Sec. 3.2], where it is introduced as one of recursively defined *Paden-Kahan* problems. An alternate way to deal with Problem 1 is to transform the 3R open chain into a closed four-bar linkage such that the analytic approach by Freudenstein and Yang [7], [25], based on a loop-closure equation, can be applied, see for example [2].
In [5], Davenport found that all orientations in $SO(3)$ can be realized by the axes' constellation, if the three axes are sequentially perpendicular ($\hat{\boldsymbol{\omega}}_1 \perp \hat{\boldsymbol{\omega}}_2$ and $\hat{\boldsymbol{\omega}}_2 \perp \hat{\boldsymbol{\omega}}_3$). Therefore, angles around such axes are called *Davenport angles* [23]. Extending this orthogonality condition, the solution space of Problem 1 was recently characterized in [20] by an inequality (see Theorem 1, here). In [16], a similar analysis was conducted using the Cayley map. In this paper, the inequality condition of [20] is extended for the following, set-generalized variant of Problem 1.

Problem 2 (Rotation Workspace)**.** *Given three rotation axes $\hat{\boldsymbol{\omega}}_1$, $\hat{\boldsymbol{\omega}}_2$, $\hat{\boldsymbol{\omega}}_3$, determine for all orientations $\boldsymbol{R} \in SO(3)$ if Equation 1 admits no, one, two, or an infinite number of solutions for the rotation angles ϕ_1, ϕ_2, and ϕ_3.*

The solution space of Problem 2 is characterized in the Theorems 2, 3, and 4 via two orthogonally interlaced toroids within a unit ball that corresponds to a double cover of $SO(3)$. The toroids represent the set of singular orientations and the workspace boundaries of the constellation of rotation axes.
The structure of this paper is as follows: in Section 2 required concepts, i.a., the *unit ball representation* of rotations, are introduced. In addition to Section 2, convenient definitions for handling angles and rotations in three dimensions are collected in an appendix at the end of the document. In Section 3, essential facts for Problem 1 are compiled first in Section 3.1. Subsequently in

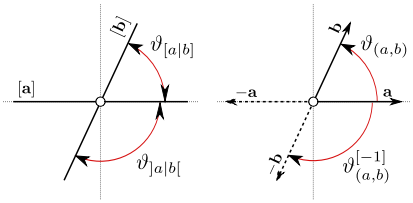

FIGURE 1. Minimal and maximal angles between axes $[\boldsymbol{a}]$ and $[\boldsymbol{b}]$; directed angles between vectors $\boldsymbol{a}$ and $\boldsymbol{b}$, and between vectors $\boldsymbol{a}$ and $-\boldsymbol{b}$.

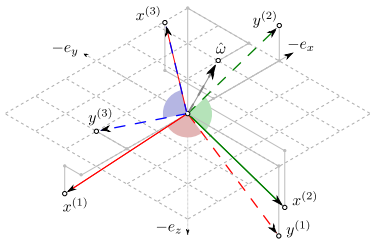

FIGURE 2. Visualizations of the matrices $-(\hat{\boldsymbol{\omega}}^{\otimes})^2$ (solid) and $\hat{\boldsymbol{\omega}}^{\otimes}$ (dashed) for axis $\hat{\boldsymbol{\omega}} = (1,2,3)^{\odot T}$.

Section 3.2, the central theorems are presented as a solution for Problem 2 together with proofs. In Section 3.3 and Section 3.4, the presented approach is supported by a set of examples and a discussion about several applications is provided. Finally, a summary is provided in Section 4.

2. Prerequisites

2.1. **Notation.** In this document, all vectors are of $\mathbb{R}^3$ and denoted by a bold letter, as $\boldsymbol{v}$. Lines passing through the origin are denoted by $[v_1 : v_2 : v_3] = [\boldsymbol{v}] = \{\kappa \cdot \boldsymbol{v} \mid \kappa \in \mathbb{R}\}$. Unit vectors are indicated by a hat, as $\hat{\boldsymbol{v}} = \frac{\boldsymbol{v}}{\|\boldsymbol{v}\|}$.

Vector Operations. The operator $^{\odot}$ scales a vector to norm one, as $\boldsymbol{v}^{\odot} = \hat{\boldsymbol{v}}$. For the concatenation of transposition and multiplication, the symbol $*$ is used, for example as $\boldsymbol{a} * \boldsymbol{b} = \boldsymbol{a}^T \cdot \boldsymbol{b}$ (according to [6]).[1] For the outer product of two identical vectors, the abbreviation $\boldsymbol{a}^{\boxtimes} = \boldsymbol{a} \cdot \boldsymbol{a}^T$ is introduced.[2] The cross operator $\times$ is generalized by the function χ in prefix notation: for two arguments, define $\chi(\boldsymbol{a},\boldsymbol{b}) := \boldsymbol{a} \times \boldsymbol{b}$. Additionally, for three arguments with repetitions, the abbreviations $\chi(\boldsymbol{a},\boldsymbol{a},\boldsymbol{b}) := \boldsymbol{a} \times (\boldsymbol{a} \times \boldsymbol{b})$ and $\chi(\boldsymbol{a},\boldsymbol{b},\boldsymbol{b}) := (\boldsymbol{a} \times \boldsymbol{b}) \times \boldsymbol{b}$ are defined. The projection of $\boldsymbol{b}$ onto $\boldsymbol{a}$ is denoted as $\pi_{\boldsymbol{a}}(\boldsymbol{b}) = \frac{\boldsymbol{b}*\boldsymbol{a}}{\boldsymbol{a}*\boldsymbol{a}} \cdot \boldsymbol{a}$, the projection of $\boldsymbol{b}$ onto $\boldsymbol{a}^{\perp}$ is denoted as $\tau_{\boldsymbol{a}}(\boldsymbol{b}) = \boldsymbol{b} - \frac{\boldsymbol{b}*\boldsymbol{a}}{\boldsymbol{a}*\boldsymbol{a}} \cdot \boldsymbol{a}$. The concatenations of the former expressions are written as $\hat{\chi}(\boldsymbol{a},\boldsymbol{b}) := (\chi(\boldsymbol{a},\boldsymbol{b}))^{\odot} = \frac{1}{\|\boldsymbol{a}\times\boldsymbol{b}\|} \cdot (\boldsymbol{a} \times \boldsymbol{b})$, as $\hat{\pi}(\boldsymbol{a},\boldsymbol{b}) := (\pi_{\boldsymbol{a}}(\boldsymbol{b}))^{\odot}$, and as $\hat{\tau}(\boldsymbol{a},\boldsymbol{b}) := (\tau_{\boldsymbol{a}}(\boldsymbol{b}))^{\odot}$. The operator $\boldsymbol{a}^{\otimes}$ assigns the associated skew-symmetric matrix to a vector $\boldsymbol{a}$ (see also Definition 1). The operator $\boldsymbol{S}^{\oplus}$ with $\boldsymbol{S} = \boldsymbol{a}^{\otimes}$ extracts the axis vector $\boldsymbol{a}$.

Angles. In this text, angles appear in different contexts. An angle is generally denoted with φ and – if not indicated otherwise – drawn from the 'principal' interval $(-\pi,\pi]$. An angle which is an argument of a *rotation* is denoted with ϕ. An angle between *vectors* or *lines* is denoted by the symbol ϑ together with a superindex reflecting the *normal axis* of the plane containing the angle measurement and a subindex reflecting the *passive interpretation*. The notation for an *undirected* angle $\vartheta^{[\hat{\boldsymbol{\omega}}]}_{|\boldsymbol{a},\boldsymbol{b}|} = \vartheta^{[\hat{\boldsymbol{\omega}}]}_{|\boldsymbol{b},\boldsymbol{a}|} \in [0,\pi]$, a *minimal* angle $\vartheta^{[\hat{\boldsymbol{\omega}}]}_{[\boldsymbol{a}|\boldsymbol{b}]} = \vartheta^{[\hat{\boldsymbol{\omega}}]}_{[\boldsymbol{b}|\boldsymbol{a}]} \in [0,\frac{\pi}{2})$, a *maximal* angle $\vartheta^{[\hat{\boldsymbol{\omega}}]}_{]\boldsymbol{a}|\boldsymbol{b}[} = \vartheta^{[\hat{\boldsymbol{\omega}}]}_{]\boldsymbol{b}|\boldsymbol{a}[} \in [\frac{\pi}{2},\pi)$,and a *directed* angle $\vartheta^{\langle\hat{\boldsymbol{\omega}}\rangle}_{(\boldsymbol{b},\boldsymbol{a})} = \overline{\vartheta}^{\langle\hat{\boldsymbol{\omega}}\rangle}_{(\boldsymbol{a},\boldsymbol{b})} \in (-\pi,\pi]$, is introduced in Definitions 6, 7, and 10 in Appendix A. In Figure 1, examples are provided.

An overview about the used notation conventions is given in Appendix D.

2.2. **Orthogonal Decomposition of Rotation Matrices.** By means of the two following definitions, product terms of the form $\boldsymbol{a} * \boldsymbol{X} \cdot \boldsymbol{b}$, with $\boldsymbol{X}$ as placeholder for one of the matrices $\hat{\boldsymbol{\omega}}^{\otimes}$, $-(\hat{\boldsymbol{\omega}}^{\otimes})^2$, $\hat{\boldsymbol{\omega}}^{\boxtimes}$, $\boldsymbol{R} - \hat{\boldsymbol{\omega}}^{\boxtimes}$, $\boldsymbol{R}$, are simplified below. The derived simplifications will be used in the remainder of the document.

[1] Gibbs' notation $\boldsymbol{a} \cdot \boldsymbol{b} := \sum_k a_k \cdot b_k$ does not comply with matrix multiplication. The short notation $\boldsymbol{a}^T\boldsymbol{b} := \boldsymbol{a}^T \cdot \boldsymbol{b}$ (juxtaposition) might imply the impression of an unary instead of a binary operation and tends to introduce redundant parentheses. See [13] about the history of denoting vector arithmetics.

[2] The symbol $^{\boxtimes}$ reflects the quadratic shape of a matrix combined with a stylized version of the symbol '2' ('squared').

Definition 1 (Generators of '$\hat{\boldsymbol{\omega}}^{\perp}$')**.** For a unit vector $\hat{\boldsymbol{\omega}}$, (i) the *skew-symmetric* matrix $\hat{\boldsymbol{\omega}}^{\otimes}$ is defined as

$$\hat{\boldsymbol{\omega}}^{\otimes} = \begin{pmatrix} 0 & -\hat{\omega}_3 & \hat{\omega}_2 \\ \hat{\omega}_3 & 0 & -\hat{\omega}_1 \\ -\hat{\omega}_2 & \hat{\omega}_1 & 0 \end{pmatrix},$$

and, (ii) the *symmetric* matrix $-(\hat{\boldsymbol{\omega}}^{\otimes})^2$ is defined as

$$-(\hat{\boldsymbol{\omega}}^{\otimes})^2 = \begin{pmatrix} \hat{\omega}_2^2+\hat{\omega}_3^2 & -\hat{\omega}_1*\hat{\omega}_2 & -\hat{\omega}_1*\hat{\omega}_3 \\ -\hat{\omega}_1*\hat{\omega}_2 & \hat{\omega}_1^2+\hat{\omega}_3^2 & -\hat{\omega}_2*\hat{\omega}_3 \\ -\hat{\omega}_1*\hat{\omega}_3 & -\hat{\omega}_2*\hat{\omega}_3 & \hat{\omega}_1^2+\hat{\omega}_2^2 \end{pmatrix}.$$

By definition, the column vectors of $\hat{\boldsymbol{\omega}}^{\otimes}$ and the column vectors of $-(\hat{\boldsymbol{\omega}}^{\otimes})^2$ lie in the plane $\hat{\boldsymbol{\omega}}^{\perp}$ orthogonal to $\hat{\boldsymbol{\omega}}$. For an illustration, see the vectors $\left(\boldsymbol{x}^{(1)}\,\boldsymbol{x}^{(2)}\,\boldsymbol{x}^{(3)}\right) := -(\hat{\boldsymbol{\omega}}^{\otimes})^2$, and $\left(\boldsymbol{y}^{(1)}\,\boldsymbol{y}^{(2)}\,\boldsymbol{y}^{(3)}\right) := \hat{\boldsymbol{\omega}}^{\otimes}$ in Figure 2. Using the three identities $\omega_j^2+\omega_k^2 = 1-\omega_l^2$, where $\{j,k,l\}$ are the cyclic permutations of $\{1,2,3\}$, one can show that $\|\boldsymbol{y}^{(i)}\| = \|\boldsymbol{x}^{(i)}\|$ for $1 \le i \le 3$. By definition, it holds that $\boldsymbol{y}^{(i)} \perp \boldsymbol{x}^{(i)}$ for $1 \le i \le 3$, and, in particular, it holds that $\hat{\boldsymbol{\omega}}^{\otimes}$ is a 'front-rotated' version of $-(\hat{\boldsymbol{\omega}}^{\otimes})^2$ with respect to $\hat{\boldsymbol{\omega}}$, in the sense of $\hat{\boldsymbol{\omega}}^{\otimes} = \boldsymbol{R}(\frac{\pi}{2};\hat{\boldsymbol{\omega}})\cdot(-(\hat{\boldsymbol{\omega}}^{\otimes})^2) = (-(\hat{\boldsymbol{\omega}}^{\otimes})^2)\cdot\boldsymbol{R}(\frac{\pi}{2};\hat{\boldsymbol{\omega}})$.

Definition 2 (Projections of 'exp')**.** For a given tangential vector $\phi\cdot\hat{\boldsymbol{\omega}}^{\otimes} \in so(3)$ (see Appendix B), define (i) the *normal* exponential map 'nexp' as the map

$$\mathrm{nexp}(\phi\cdot\hat{\boldsymbol{\omega}}^{\otimes}) := \left(\left((\phi\cdot\hat{\boldsymbol{\omega}}^{\otimes})^{\oplus}\right)^{\circ}\right)^{\boxtimes} = \hat{\boldsymbol{\omega}}^{\boxtimes},$$

and, (ii) the *planar* exponential map 'pexp' as

$$\mathrm{pexp}(\phi\cdot\hat{\boldsymbol{\omega}}^{\otimes}) := \exp(\phi\cdot\hat{\boldsymbol{\omega}}^{\otimes}) - \mathrm{nexp}(\phi\cdot\hat{\boldsymbol{\omega}}^{\otimes}) \quad .$$

These definitions have alternate formulations reusing the projection operators π and τ (see Section 2.1, above) and the argument $\boldsymbol{R}$ instead of $\phi\cdot\hat{\boldsymbol{\omega}}^{\otimes}$: the normal projection of a rotation matrix $\boldsymbol{R}$ reads as $\pi_{\hat{\boldsymbol{\omega}}}(\boldsymbol{R}) \equiv \mathrm{nexp}(\phi\cdot\hat{\boldsymbol{\omega}}^{\otimes})$ and the planar projection of a rotation reads as $\tau_{\hat{\boldsymbol{\omega}}}(\boldsymbol{R}) = \boldsymbol{R} - \pi_{\hat{\boldsymbol{\omega}}}(\boldsymbol{R}) \equiv \exp(\phi\cdot\hat{\boldsymbol{\omega}}^{\otimes}) - \mathrm{nexp}(\phi\cdot\hat{\boldsymbol{\omega}}^{\otimes})$. In the remainder of the document, also, the brief notation $\boldsymbol{R}_{\Omega}(\phi;\hat{\boldsymbol{\omega}}) := \tau_{\hat{\boldsymbol{\omega}}}(\boldsymbol{R}) = \mathrm{pexp}(\phi\cdot\hat{\boldsymbol{\omega}}^{\otimes})$, with $\Omega := \hat{\boldsymbol{\omega}}^{\perp}$, will be used.

Since the value of the map 'nexp' to $\hat{\boldsymbol{\omega}}^{\boxtimes}$ is independent of ϕ, the normal part of a rotation is invariant with respect to all rotations along that axis. The planar projection rotation $\boldsymbol{R}_{\Omega} = \mathrm{pexp}(\phi\cdot\hat{\boldsymbol{\omega}}^{\otimes}) = \exp(\phi\cdot\hat{\boldsymbol{\omega}}^{\otimes}) - \hat{\boldsymbol{\omega}}^{\boxtimes}$ can be reformulated by applying the Rodrigues' formula (Equation B.2) for $\exp(\phi\cdot\hat{\boldsymbol{\omega}}^{\otimes})$ and the identity[3] $\hat{\boldsymbol{\omega}}^{\boxtimes} = \boldsymbol{I} + (\hat{\boldsymbol{\omega}}^{\otimes})^2$ for $\hat{\boldsymbol{\omega}}^{\boxtimes}$ to reach a *'planar'* variant of Rodrigues formula as

$$\boldsymbol{R}_{\Omega}(\phi) = \cos\phi\cdot(-(\hat{\boldsymbol{\omega}}^{\otimes})^2) + \sin\phi\cdot\hat{\boldsymbol{\omega}}^{\otimes}. \tag{2}$$

In other words, the planar exponential function $\mathrm{pexp}(\phi\cdot\hat{\boldsymbol{\omega}}^{\otimes})$ is the exponential function substracted by the 'aligned one' $\hat{\boldsymbol{\omega}}^{\boxtimes}$, passing zero.[4] A rotation matrix $\boldsymbol{R} = \exp(\phi\cdot\hat{\boldsymbol{\omega}}^{\otimes})$ can be transformed by means of the two precedent definitions of its axial and its planar component to[5]

$$\begin{aligned} \exp(\phi\cdot\hat{\boldsymbol{\omega}}^{\otimes}) &= \mathrm{pexp}(\phi\cdot\hat{\boldsymbol{\omega}}^{\otimes}) + \mathrm{nexp}(\phi\cdot\hat{\boldsymbol{\omega}}^{\otimes}) \\ &= \boldsymbol{R}(\phi,\hat{\boldsymbol{\omega}}) = \boldsymbol{R}_{\Omega}(\phi,\hat{\boldsymbol{\omega}}) + \hat{\boldsymbol{\omega}}^{\boxtimes}. \end{aligned} \tag{3}$$

---

[3] The equality $\hat{\boldsymbol{\omega}}^{\boxtimes} = \boldsymbol{I} + (\hat{\boldsymbol{\omega}}^{\otimes})^2$ holds for unit vectors as a special case of the general $\boldsymbol{a}^{\boxtimes} = \|\boldsymbol{a}\|^2\cdot(\boldsymbol{I} + (\hat{\boldsymbol{a}}^{\otimes})^2)$.

[4] The 'planar' exponential function 'pexp' is the proper generalization of the 'planar' exponential formula for (pure) complex numbers, $\exp(i\cdot\varphi) = \cos(\varphi) + i\cdot\sin(\varphi)$, for arbitrary planes in three dimensions. This becomes obvious, when the latter is given in matrix form as $\exp(i\cdot\varphi) = \cos\varphi\cdot\begin{pmatrix} 1 & 0 & 0 \\ 0 & 1 & 0 \\ 0 & 0 & 0 \end{pmatrix} + \sin\varphi\cdot\begin{pmatrix} 0 & -1 & 0 \\ 1 & 0 & 0 \\ 0 & 0 & 0 \end{pmatrix}$ with $\hat{\boldsymbol{\omega}} = (0,0,1)^T$ (see, for example [24]).

[5] Expanding Equation 3 by Equation 2, a *variant* of the *exponential formula* for $\boldsymbol{R}$ is derived with $\boldsymbol{R}(\phi,\hat{\boldsymbol{\omega}}) = \cos\phi\cdot(-(\hat{\boldsymbol{\omega}}^{\otimes})^2) + \sin\phi\cdot\hat{\boldsymbol{\omega}}^{\otimes} + \hat{\boldsymbol{\omega}}^{\boxtimes}$. In this formulation, a rotation matrix $\boldsymbol{R}$ is expressed as a 'spherical-affine combination' of the three 'basis matrices' $(-(\hat{\boldsymbol{\omega}}^{\otimes})^2)$, $\hat{\boldsymbol{\omega}}^{\otimes}$ and $\hat{\boldsymbol{\omega}}^{\boxtimes}$.

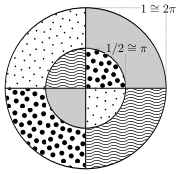

FIGURE 3. Corresponding areas of principal and secondary rotation vectors in a planar slice of the unit ball representation.

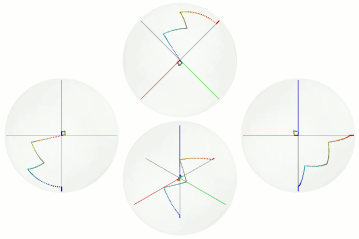

(A) Chain of orientations $\mathcal{R}$ in unit ball representation; views from (i) *left*, $(1,0,0)^T$, (ii) *slanted above*, $(1,1,1)^T$, (iii) *right*, $(0,1,0)^T$, and (iv) *top*, $(0,0,1)^T$, counterclockwise.

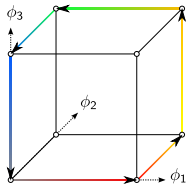

(B) Chain of orientations $\mathcal{R}$ in Euler angle representation.

FIGURE 4. Example of a closed sequence of orientations $\mathcal{R}$ in unit ball and Euler angle representation.

Applications. Using the abbrevation $\boldsymbol{v}_\Omega := \tau_{\hat{\boldsymbol{\omega}}}(\boldsymbol{v})$, the bilinear product of a symmetric matrix $-(\hat{\boldsymbol{\omega}}^\otimes)^2$ (Definition 1) with two vectors $\boldsymbol{a}$ and $\boldsymbol{b}$ reads as

$$\boldsymbol{a} * (-(\hat{\boldsymbol{\omega}}^\otimes)^2) \cdot \boldsymbol{b} = \boldsymbol{a}_\Omega * \boldsymbol{b}_\Omega = \cos \vartheta^{\langle\hat{\boldsymbol{\omega}}\rangle}_{(\boldsymbol{a},\boldsymbol{b})} \cdot \|\boldsymbol{a}_\Omega\| \cdot \|\boldsymbol{b}_\Omega\| \,. \tag{4}$$

Similarly, the product of a skew-symmetric matrix $\hat{\boldsymbol{\omega}}^\otimes$ (Definition 1) with two vectors $\boldsymbol{a}$ and $\boldsymbol{b}$ reads as

$$\begin{aligned} \boldsymbol{a} * \hat{\boldsymbol{\omega}}^\otimes \cdot \boldsymbol{b} = \boldsymbol{a} * (\hat{\boldsymbol{\omega}} \times \boldsymbol{b}) &= \cos \vartheta^{\langle\hat{\boldsymbol{\omega}}\rangle}_{(\boldsymbol{a},\hat{\boldsymbol{\omega}}\times\boldsymbol{b})} \cdot \|\boldsymbol{a}_\Omega\| \cdot \|\hat{\boldsymbol{\omega}} \times \boldsymbol{b}\| \\ &= -\sin \vartheta^{\langle\hat{\boldsymbol{\omega}}\rangle}_{(\boldsymbol{a},\boldsymbol{b})} \cdot \|\boldsymbol{a}_\Omega\| \cdot \|\boldsymbol{b}_\Omega\| \,. \end{aligned} \tag{5}$$

The last equation follows using the 'front-rotated' argument above. Using the abbreviation $\boldsymbol{v}_{\hat{\boldsymbol{\omega}}} := \pi_{\hat{\boldsymbol{\omega}}}(\boldsymbol{v})$, the bilinear product of the axial component of a rotation $\hat{\boldsymbol{\omega}}^{\boxslash}$ (Definition 2) with two vectors $\boldsymbol{a}$ and $\boldsymbol{b}$ reads as

$$\boldsymbol{a} * \hat{\boldsymbol{\omega}}^{\boxslash} \cdot \boldsymbol{b} = \boldsymbol{a}_{\hat{\boldsymbol{\omega}}} * \boldsymbol{b}_{\hat{\boldsymbol{\omega}}} \,. \tag{6}$$

Similarly, the product of the planar component of a rotation $\boldsymbol{R}_\Omega$ with two vectors $\boldsymbol{a}$ and $\boldsymbol{b}$ reads as

$$\boldsymbol{a} * (\boldsymbol{R}(\phi;\hat{\boldsymbol{\omega}}) - \hat{\boldsymbol{\omega}}^{\boxslash}) \cdot \boldsymbol{b} = \boldsymbol{a} * \boldsymbol{R}_\Omega(\phi) \cdot \boldsymbol{b} = \boldsymbol{a}_\Omega * \boldsymbol{R}_\Omega(\phi) \cdot \boldsymbol{b}_\Omega \,. \tag{7}$$

Finally, the bilinear product of a rotation matrix $\boldsymbol{R}$ with two vectors $\boldsymbol{a}$ and $\boldsymbol{b}$ can be transformed, using Equation 3, Equation 6, and Equation 7, to

$$\begin{aligned} \boldsymbol{a} * \boldsymbol{R}(\phi,\hat{\boldsymbol{\omega}}) \cdot \boldsymbol{b} &= \boldsymbol{a} * \boldsymbol{R}_\Omega(\phi,\hat{\boldsymbol{\omega}}) \cdot \boldsymbol{b} + \boldsymbol{a} * (\hat{\boldsymbol{\omega}}^{\boxslash}) \cdot \boldsymbol{b} \\ &= \boldsymbol{a}_\Omega * \boldsymbol{R}_\Omega(\phi,\hat{\boldsymbol{\omega}}) \cdot \boldsymbol{b}_\Omega + \boldsymbol{a}_{\hat{\boldsymbol{\omega}}} * \boldsymbol{b}_{\hat{\boldsymbol{\omega}}} \,. \end{aligned} \tag{8}$$

In Appendices A and B, further aspects of angles and rotations, i.a., their *passive* and their *active* interpretation, are compiled.

2.3. **Unit Ball Representation.** The remainder of this document is based on the following representation of rotations, where *two* vectors $\boldsymbol{v}'$ and $\boldsymbol{v}''$ inside the unit ball $\mathcal{B}^3(1)$ are assigned to *one* rotation $\boldsymbol{R} \in SO(3)$ by the mapping $v^\star$.

Definition 3 (Dualization)**.** Given a (primal) angle $\varphi \in (-\pi,\pi]$, the *dual* angle $\varphi'' \in (-2\pi,2\pi] \setminus (-\pi,\pi]$ is defined, with $\operatorname{sign}^\star$ according to Definition 9, as

$$\varphi'' := \varphi + \operatorname{sign}^\star(-\varphi) \cdot 2\pi \,.$$

The *dualization* corresponds to a 'shift into the outer shell', see Figure 3 for a planar illustration.

Definition 4 (Unit Ball Representation)**.** Given a rotation as $\boldsymbol{R} = \boldsymbol{R}(\phi;\hat{\boldsymbol{\omega}}) = \boldsymbol{R}(\phi'';\hat{\boldsymbol{\omega}})$ (with $\phi \in (-\pi,\pi]$ and ϕ'' according to Definition 3), the tuple $v^\star = v^\star(\boldsymbol{R}) = \left(\boldsymbol{v}',\boldsymbol{v}''\right)$ of *rotation vectors* $\boldsymbol{v}'$ and $\boldsymbol{v}''$ is defined by

$$\boldsymbol{v}'(\phi,\hat{\boldsymbol{\omega}}) = \frac{1}{2\pi} \cdot \phi \cdot \hat{\boldsymbol{\omega}} \in \mathcal{B}^3(\tfrac{1}{2}) \qquad\qquad \boldsymbol{v}''(\phi'',\hat{\boldsymbol{\omega}}) = \frac{1}{2\pi} \cdot \phi'' \cdot \hat{\boldsymbol{\omega}} \in \mathcal{B}^3(1) \setminus \mathcal{B}^3(\tfrac{1}{2}) \,.$$

This definition uses a 'renormed, principal' rotation vector ($|\varphi| \leq \pi$, see [3]) together with 'secondary' rotation vector ($\pi < |\varphi''| \leq 2\pi$) resulting in a double cover of $SO(3)$ (see Figure 3), as for quaternions. In particular, the unit ball represention is *equivalent* to the representation via quaternions, as shown in Appendix C. In contrast to those, [9], the unit ball representation allows a straightforward visualization due to its reduced dimension. The relation of the unit ball representation to Euler angles is illustrated in the following *example*: In Figure 4, two views on a chain of orientions $\mathcal{R}$ are provided. The set $\mathcal{R}$ is defined via the 'restricted' ramp function $\alpha_k^\Delta(x) := \left\{ \begin{smallmatrix} 0 & x < k\cdot\Delta \\ x-k\cdot\Delta & k\cdot\Delta \leq x < (k+1)\cdot\Delta \\ \Delta & (k+1)\cdot\Delta < x \end{smallmatrix} \right.$ and its complementary function $\overline{\alpha}^\Delta$ as $\overline{\alpha}_k^\Delta(x) = \Delta - \alpha_k^\Delta(x)$. With those two, the set of orientations reads $\mathcal{R} = \Big\{ \boldsymbol{R} \;\Big|\; \boldsymbol{R} = \boldsymbol{R}_z\big(\alpha_0^\Delta(\varphi)\big)\cdot\boldsymbol{R}_x(\alpha_1^\Delta(\varphi))\cdot\boldsymbol{R}_z(\alpha_2^\Delta(\varphi))\cdot \boldsymbol{R}_z(\overline{\alpha}_3^\Delta(\varphi))\cdot\boldsymbol{R}_x(\overline{\alpha}_4^\Delta(\varphi))\cdot\boldsymbol{R}_z(\overline{\alpha}_5^\Delta(\varphi)),\ 0 \leq \varphi \leq 6\cdot\Delta \Big\}$. Contrary to Euler angles, the densitiy of (not only) this vectorial representation is independent of the rotation axis and thus symmetric to identity [1].

3. Spatial Analysis

3.1. Decomposition for One Orientation.

The *number of solutions* for Problem 1 – the number of angle configurations for a given constellation of non-orthogonal axes (for an example see Figure 5) and a target orientation – was characterized in [20] by the following theorem.

Theorem 1 (Number of Solutions)**.** *The number of solution triplets (ϕ_1, ϕ_2, ϕ_3) for Problem 1 is determined by the inequality*

$$|\hat{\boldsymbol{\omega}}_1 * (\boldsymbol{R} - \hat{\boldsymbol{\omega}}_2^{\boxtimes}) \cdot \hat{\boldsymbol{\omega}}_3| \leq \|\boldsymbol{\omega}_{1\perp 2}\| \cdot \|\boldsymbol{\omega}_{3\perp 2}\| \,, \tag{9}$$

with $\hat{\boldsymbol{\omega}}_{i\perp j} := \hat{\tau}_{\hat{\boldsymbol{\omega}}_i}(\hat{\boldsymbol{\omega}}_j)$. If Inequality 9 is strictly fulfilled, two solutions (ϕ_1, ϕ_2, ϕ_3) exist. If Inequality 9 is fulfilled with equality, only one solution exists for ϕ_2. If Inequality 9 is not fulfilled, no solution exists. ϕ_1 and ϕ_3 are determined in dependence on ϕ_2.

The following chain of equalities outlines the idea of the proof of the theorem (see [20]) by using the notation introduced in Section 2.

$$\begin{aligned}
&\left|\hat{\boldsymbol{\omega}}_1 * (\boldsymbol{R} - \hat{\boldsymbol{\omega}}_2^{\boxtimes}) \cdot \hat{\boldsymbol{\omega}}_3\right| \\
&\overset{\text{(i)}}{=} \left|\hat{\boldsymbol{\omega}}_1 * (\boldsymbol{R}_1(\phi_1)\cdot\boldsymbol{R}_2(\phi_2)\cdot\boldsymbol{R}_3(\phi_3)) \cdot \hat{\boldsymbol{\omega}}_3 - \hat{\boldsymbol{\omega}}_1 * \hat{\boldsymbol{\omega}}_2^{\boxtimes} \cdot \hat{\boldsymbol{\omega}}_3\right| \\
&\overset{\text{(ii)}}{=} \left|\hat{\boldsymbol{\omega}}_1 * \boldsymbol{R}_2(\phi_2) \cdot \hat{\boldsymbol{\omega}}_3 - \hat{\boldsymbol{\omega}}_1 * \hat{\boldsymbol{\omega}}_2^{\boxtimes} \cdot \hat{\boldsymbol{\omega}}_3\right| \\
&= \left|\hat{\boldsymbol{\omega}}_1 * (\boldsymbol{R}_2(\phi_2) - \hat{\boldsymbol{\omega}}_2^{\boxtimes}) \cdot \hat{\boldsymbol{\omega}}_3\right| \\
&\overset{\text{(iii)}}{=} \left|\boldsymbol{\omega}_{1\perp 2} * \boldsymbol{R}_{\perp 2}(\phi_2) \cdot \boldsymbol{\omega}_{3\perp 2}\right| \\
&\leq \|\boldsymbol{\omega}_{1\perp 2}\| \cdot \|\boldsymbol{\omega}_{3\perp 2}\|
\end{aligned} \tag{10}$$

Equality (i) incorporates the claim for a feasible angle configuration for $\boldsymbol{R}$. For Equality (ii), the invariance of rotations along their axes is used. Equality (iii) follows with Equation 7 for the planar rotation $\boldsymbol{R}_{\perp 2}(\phi_2) := \tau_{\hat{\boldsymbol{\omega}}_2}(\boldsymbol{R}_2)$ (Definition 2).

Computation of Angle Configurations. For sake of completeness, and since similar steps are conducted in the proof of Theorem 2 in Section 3.2, the computation of angle configurations is recapitulated in the following by means of the compact notation from Section 2 and Appendix A. To determine the angles ϕ_1, ϕ_2, and ϕ_3, the ansatz in [20] and [16] is given by the observation $\hat{\boldsymbol{\omega}}_1 * \boldsymbol{R}_1 \cdot \boldsymbol{R}_2 \cdot \boldsymbol{R}_3 \cdot \hat{\boldsymbol{\omega}}_3 = \hat{\boldsymbol{\omega}}_1 * \boldsymbol{R}_2 \cdot \hat{\boldsymbol{\omega}}_3$. Applying the exponential map (Equation B.2) to $\boldsymbol{R}_2$ results in $\hat{\boldsymbol{\omega}}_1 * \boldsymbol{R} \cdot \hat{\boldsymbol{\omega}}_3 = \hat{\boldsymbol{\omega}}_1 * \big(\boldsymbol{I} + \sin\phi_2 \cdot \hat{\boldsymbol{\omega}}_2^{\otimes} + (1-\cos\phi_2)\cdot(\hat{\boldsymbol{\omega}}_2^{\otimes})^2\big) \cdot \hat{\boldsymbol{\omega}}_3$. This equation is resorted and redefined by means of

$$a := \hat{\boldsymbol{\omega}}_1 * (-(\hat{\boldsymbol{\omega}}_2^{\otimes})^2) \cdot \hat{\boldsymbol{\omega}}_3 \qquad b := \hat{\boldsymbol{\omega}}_1 * \hat{\boldsymbol{\omega}}_2^{\otimes} \cdot \hat{\boldsymbol{\omega}}_3 \qquad c := \hat{\boldsymbol{\omega}}_1 * \big(\boldsymbol{R} - \hat{\boldsymbol{\omega}}_2^{\boxtimes}\big) \cdot \hat{\boldsymbol{\omega}}_3$$

to reach the equation

$$a \cdot \cos\phi_2 + b \cdot \sin\phi_2 = c \,. \tag{11}$$

This equation is of the form $a\cdot\cos\varphi + b\cdot\sin\varphi = c$ and has the two solutions

$$\varphi_{1,2} = \operatorname{atan}\frac{b}{a} \pm \operatorname{atan}\frac{d}{c} \quad \text{with} \quad d = \sqrt{a^2+b^2-c^2},$$

which coincide for $d = 0$. For convenience, the definitions

$$\phi_{2^0} := \operatorname{atan}_2^\star \frac{b}{a} \qquad\qquad \phi_{2^\Delta} := \operatorname{atan}_2^\star \frac{d}{c} \ ,$$

are introduced and simplified. First, for a and b, by means of using Equation 4 and Equation 5, it can be shown that

$$\begin{aligned} a &= +\cos\vartheta^{\langle 2\rangle}_{(1,3)} \cdot \|\boldsymbol{\omega}_{1\perp 2}\| \cdot \|\boldsymbol{\omega}_{3\perp 2}\| \\ b &= -\sin\vartheta^{\langle 2\rangle}_{(1,3)} \cdot \|\boldsymbol{\omega}_{1\perp 2}\| \cdot \|\boldsymbol{\omega}_{3\perp 2}\| \ . \end{aligned}$$

Taking into account Equations A.1, A.2, and A.5, the expression $\phi_{2^0} = \operatorname{atan}_2^\star \frac{b}{a}$ is transformed to

$$\phi_{2^0} = \operatorname{atan}_2^\star \frac{b}{a} = \operatorname{atan}_2^\star \frac{-\sin\vartheta^{\langle 2\rangle}_{(1,3)}}{\cos\vartheta^{\langle 2\rangle}_{(1,3)}} = \operatorname{acos}_3^\star\big(\hat{\boldsymbol{\omega}}_1, \hat{\boldsymbol{\omega}}_3; -\hat{\boldsymbol{\omega}}_2\big) = \vartheta^{\langle 2\rangle}_{(1,3)} \ . \tag{12}$$

Second, to simplify the expression $\operatorname{atan}_2^\star \frac{d}{c}$, an auxiliary variable c' is defined as $c' := \frac{c}{\|\boldsymbol{\omega}_{1\perp 2}\|\cdot\|\boldsymbol{\omega}_{1\perp 2}\|}$ for which the equation

$$c' = \hat{\boldsymbol{\omega}}_{1\perp 2} * \boldsymbol{R}(\phi_2; \hat{\boldsymbol{\omega}}_2) \cdot \hat{\boldsymbol{\omega}}_{3\perp 2} \ ,$$

holds. By means of c', the argument of $\operatorname{atan}_2^\star$, the fraction $\frac{d}{c}$, is rewritten as

$$\frac{d}{c} = \frac{\sqrt{\|\boldsymbol{\omega}_{1\perp 2}\|^2 \cdot \|\boldsymbol{\omega}_{3\perp 2}\|^2 - c^2}}{c} = \frac{\sqrt{1-(c')^2}}{c'} \ .$$

Then, with Equation A.4, the expression for $\phi_{2^\Delta} = \operatorname{atan}_2^\star \frac{d}{c}$ is transformed to

$$\phi_{2^\Delta} = \operatorname{atan}_2^\star \frac{d}{c} = \operatorname{atan}_2^\star \frac{\sqrt{1-(c')^2}}{c'} = \operatorname{acos} c' =: |\gamma'| \ .$$

Together, ϕ_{2^+} and ϕ_{2^-} are computed as

$$\phi_{2^+}, \phi_{2^-} = \phi_{2^0} \pm \phi_{2^\Delta} = \vartheta^{\langle 2\rangle}_{(1,3)} \pm |\gamma'| \ .$$

For *generic* constellations of rotation axes, with $\vartheta_{[1|2]} \neq \vartheta_{[2|3]}$, the angles ϕ_1 and ϕ_3 are computed for each of the $\phi_2 \in \big\{\, \phi_{2^+}, \phi_{2^-} \,\big\}$ as

$$\begin{aligned} \phi_1 &= \operatorname{acos}_3^\star\big(\boldsymbol{R}\cdot\hat{\boldsymbol{\omega}}_3, \boldsymbol{R}_2\cdot\hat{\boldsymbol{\omega}}_3; -\hat{\boldsymbol{\omega}}_1\big) \\ \phi_3 &= \operatorname{acos}_3^\star\big(\boldsymbol{R}^T\cdot\hat{\boldsymbol{\omega}}_1, \boldsymbol{R}_2^T\cdot\hat{\boldsymbol{\omega}}_1; +\hat{\boldsymbol{\omega}}_3\big) \ , \end{aligned}$$

by letting $\boldsymbol{R}_2 := \boldsymbol{R}(\phi_2, \hat{\boldsymbol{\omega}}_2)$. In case of singular orientations, the two solutions triplets coincide since it is $\phi_{2^+} = \phi_{2^-}$ (see next section).
For *symmetric* constellations of rotation axes, with $\vartheta_{[1|2]} = \vartheta_{[2|3]}$, and *singular* orientations with $\hat{\boldsymbol{\omega}}_1 * \boldsymbol{R}\cdot\hat{\boldsymbol{\omega}}_3 = \pm 1$, the angles ϕ_1 and ϕ_3 are determined partially via the equations

$$\phi_3 \pm \phi_1 = \operatorname{acos}_3^\star\big(\boldsymbol{R}^T\cdot\hat{\boldsymbol{\omega}}_2, \boldsymbol{R}_2^T\cdot\hat{\boldsymbol{\omega}}_2; +\hat{\boldsymbol{\omega}}_3\big) \ .$$

3.2. **Decomposition for All Orientations.** In this section, the solution of Problem 2 is presented as a generalization of Theorem 1 for Problem 1. This means, that *all* singular orientations $\boldsymbol{R}$ are determined that fulfill Inequality 9 with equality, or equivalently, by setting $\hat{\boldsymbol{\omega}}_{\mathsf{i}\|\mathsf{j}} := \hat{\pi}_{\hat{\boldsymbol{\omega}}_\mathsf{i}}(\hat{\boldsymbol{\omega}}_\mathsf{j})$,

$$\big|\, (\hat{\boldsymbol{\omega}}_1 * \boldsymbol{R}\cdot\hat{\boldsymbol{\omega}}_3) - \|\boldsymbol{\omega}_{1\|2}\| \cdot \|\boldsymbol{\omega}_{3\|2}\| \,\big| = \|\boldsymbol{\omega}_{1\perp 2}\| \cdot \|\boldsymbol{\omega}_{3\perp 2}\| \ .$$

For the subsequent analysis, generic axes with angles $0 \neq \vartheta_{[1|2]} \neq \vartheta_{[2|3]} \neq 0$ are assumed ($\vartheta_{[\mathsf{i}|\mathsf{j}]}$ denotes the minimal angle between the lines $[\hat{\boldsymbol{\omega}}_\mathsf{i}]$ and $[\hat{\boldsymbol{\omega}}_\mathsf{j}]$, see Definition 7). Special cases are mentioned later in Section 3.3. With Theorem 2, the singular solution space is characterized as toroids and the *poses* (positions and orientations) of these are specified with respect to the rotation axes $\hat{\boldsymbol{\omega}}_1$, $\hat{\boldsymbol{\omega}}_2$, and $\hat{\boldsymbol{\omega}}_3$. The proof is based on the solution of two specific *inverse* problems of Problem 1. In Theorem 3, it is shown that the two singular toroids are mutually *orthogonal*. Finally, the

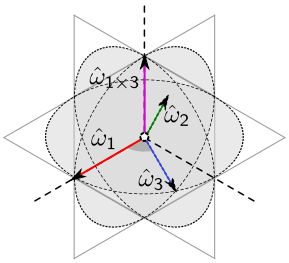

FIGURE 5. Example constellation of non-orthogonal axes $\hat{\boldsymbol{\omega}}_1 = (1{,}0{,}0)^T$, $\hat{\boldsymbol{\omega}}_2 = (1{,}2{,}3)^{\circledcirc T}$, and $\hat{\boldsymbol{\omega}}_3 = (1{,}2{,}0)^{\circledcirc T}$, together with $\hat{\boldsymbol{\omega}}_{\times 13} = (0{,}0{,}1)^T$.

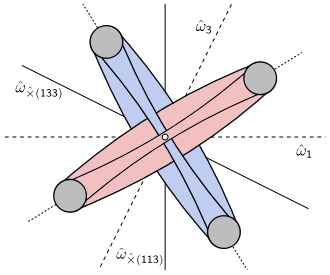

FIGURE 6. Planar sketch of two toroids viewed from $\hat{\boldsymbol{\omega}}_{\times 13} = (0{,}0{,}1)^T$. The toroids' shapes are modified to visualize the order of the mutual interlacing.

cross sectional *radii* along $\hat{\boldsymbol{\omega}}_{\times 13}$ and the *distances* to identity are determined for the two toroids in Theorem 4.

Theorem 2 (Toroids and Axes)**.** *Given an instance of Problem 2 with singular angle ϕ_{20} (Equation 12) and its inverse angle $\phi_{20}^{[-1]}$ (Definition 11), define $\phi_2^{[+]} := \phi_{20}$ and $\phi_2^{[-]} := \phi_{20}^{[-1]}$, and corresponding rotations $\boldsymbol{R}_2^{[+]} := \boldsymbol{R}(\phi_2^{[+]}, \hat{\boldsymbol{\omega}}_2)$ and $\boldsymbol{R}_2^{[-]} := \boldsymbol{R}(\phi_2^{[-]}, \hat{\boldsymbol{\omega}}_2)$. With $v^\star(\boldsymbol{R})$ according to Definition 4, define the following set of rotation vectors:*

$$\mathcal{T}^{[+]} := \left\{ v^\star(\boldsymbol{R}) \in \mathcal{B}^3 \;\middle|\; \boldsymbol{R} = \boldsymbol{R}_1(\phi_1) \cdot \boldsymbol{R}_2^{[+]} \cdot \boldsymbol{R}_3(\phi_3) \right\}$$
$$\mathcal{T}^{[-]} := \left\{ v^\star(\boldsymbol{R}) \in \mathcal{B}^3 \;\middle|\; \boldsymbol{R} = \boldsymbol{R}_1(\phi_1) \cdot \boldsymbol{R}_2^{[-]} \cdot \boldsymbol{R}_3(\phi_3) \right\},$$

where in both cases, ϕ_1 and ϕ_3 are from $(-\pi, \pi]$. The sets $\mathcal{T}^{[+]}$ and $\mathcal{T}^{[-]}$ feature the following properties:

1. *The sets $\mathcal{T}^{[+]}$ and $\mathcal{T}^{[-]}$ are toroids and represent all singular orientations.*
2. *The line $[\hat{\boldsymbol{\omega}}_2]$ is a tangent to both toroids and touches $\mathcal{T}^{[+]}$ in the boundary points $v^\star(\boldsymbol{R}_2^{[+]})$ and $\mathcal{T}^{[-]}$ in the boundary points $v^\star(\boldsymbol{R}_2^{[-]})$.*
3. *The lines $[\hat{\boldsymbol{\omega}}_1]$ and $[\hat{\boldsymbol{\omega}}_3]$ are passant (non-intersecting) lines (for short, 'passants') of $\mathcal{T}^{[+]}$ and $\mathcal{T}^{[-]}$.*
4. *The line $[\hat{\boldsymbol{\omega}}_{\times 13}]$ intersects (i) with the interior of $\mathcal{T}^{[+]}$ in $m^{[+]} := \phi_{\times 13}^{[+]0} = \vartheta_{(1,3)}^{\langle 1\times 3\rangle}$ (Equation 13, below) and in its dual angle $(m^{[+]})''$, (ii) with the interior of $\mathcal{T}^{[-]}$ in $m^{[-]} := \phi_{\times 13}^{[-]0} = (\phi_{\times 13}^{[+]0})^{[-1]}$ and in its dual angle $(m^{[-]})''$.*
5. *The line $[\hat{\boldsymbol{\omega}}_{\times 13}]$ intersects with each toroid $\mathcal{T}^{[+]}$ and $\mathcal{T}^{[-]}$ in four points. The toroid $\mathcal{T}^{[+]}$ is intersected at angles named as $\phi_{\times 13}^{[+]-}$ and $\phi_{\times 13}^{[+]+}$ (Equation 15, below), and their dual angles. The toroid $\mathcal{T}^{[-]}$ is intersected at angles named as $\phi_{\times 13}^{[-]-}$ and $\phi_{\times 13}^{[-]+}$ (Equation 16, below), and their dual angles.*

Proof. 1. Singular Toroids: For non-coincident axes $\hat{\boldsymbol{\omega}}_1$ and $\hat{\boldsymbol{\omega}}_3$, the sets $\mathcal{T}^{[+]}$ and $\mathcal{T}^{[-]}$ have dimension two. Since they are cyclic in both arguments, ϕ_1 and ϕ_3, they are toroids. Observing, (i) that the singularity condition $\hat{\boldsymbol{\omega}}_1 * \boldsymbol{R} \cdot \hat{\boldsymbol{\omega}}_3 = \pm 1$ only depends on the angle ϕ_2 (Equation 10), and (ii) that the singular angle $\phi_{20} = \vartheta_{(1,3)}^{\langle 2\rangle}$ (Equation 12) only depends on the rotation axes' constellation and not on the target orientation $\boldsymbol{R}$, it follows that all singular configurations are determined by the two toroids $\mathcal{T}^{[+]}$ and $\mathcal{T}^{[-]}$.
2. Tangent – Rotation Axis $\hat{\boldsymbol{\omega}}_2$. By definition, the line $[\hat{\boldsymbol{\omega}}_2]$ shares two points with toroid $\mathcal{T}^{[+]}$ and two points with toroid $\mathcal{T}^{[-]}$ ($\phi_1 = \phi_3 = 0$ and $\phi_1 = \phi_3 = \pi$). Each point on the axis $\hat{\boldsymbol{\omega}}_2$ represents an *admissible* orientation $\boldsymbol{R} = \boldsymbol{I} \cdot \boldsymbol{R}(\phi_2, \hat{\boldsymbol{\omega}}_2) \cdot \boldsymbol{I}$ of the axes' constellation. Thus, the axis $\hat{\boldsymbol{\omega}}_2$ does not pass the interior of $\mathcal{T}^{[+]}$ and $\mathcal{T}^{[-]}$ and is a *tangent* to both.

3. Passants – Rotation Axes $\hat{\boldsymbol{\omega}}_1$ and $\hat{\boldsymbol{\omega}}_3$. Each point of the line $[\hat{\boldsymbol{\omega}}_1]$ (of the line $[\hat{\boldsymbol{\omega}}_3]$) represents an *admissible*, non-singular orientation with $\boldsymbol{R} = \boldsymbol{R}(\phi_1, \hat{\boldsymbol{\omega}}_1) \cdot \boldsymbol{I} \cdot \boldsymbol{I}$ (with $\boldsymbol{R} = \boldsymbol{I} \cdot \boldsymbol{I} \cdot \boldsymbol{R}(\phi_3, \hat{\boldsymbol{\omega}}_3)$) since $c' \neq 0$ for $\phi_2 = 0$. Therefore, the axes $\hat{\boldsymbol{\omega}}_1$ and $\hat{\boldsymbol{\omega}}_3$ do not intersect with $\mathcal{T}^{[+]}$ or $\mathcal{T}^{[-]}$ and are *passants*.
4. & 5. Secant – Orthogonal Axis $\hat{\boldsymbol{\omega}}_{\times 13}$. For the angle $m^{[+]} = \vartheta^{\langle 1\times 3\rangle}_{(1,3)} = \measuredangle_{\hat{\boldsymbol{\omega}}_{\times 13}}(\hat{\boldsymbol{\omega}}_3, \hat{\boldsymbol{\omega}}_1)$ (Definition 10) define the corresponding orientation $\boldsymbol{R}^{[+]}_m := \boldsymbol{R}(m^{[+]}, \hat{\boldsymbol{\omega}}_{\times 13})$. For a generic axes' constellation with $0 \neq \vartheta_{[1|2]} \neq \vartheta_{[2|3]} \neq 0$ the $\boldsymbol{R}^{[+]}_m$ is not realizable: it holds $\boldsymbol{R}^{[+]}_m \neq \boldsymbol{R}_1(\phi_1) \cdot \boldsymbol{R}_2(\phi_2) \cdot \boldsymbol{R}_3(\phi_3)$ and according to Theorem 1 it holds

$$\left|\hat{\boldsymbol{\omega}}_1 * (\boldsymbol{R}^{[+]}_m - \hat{\boldsymbol{\omega}}^{\boxtimes}_2) \cdot \hat{\boldsymbol{\omega}}_3\right| > \|\boldsymbol{\omega}_{1\perp 2}\| \cdot \|\boldsymbol{\omega}_{3\perp 2}\| \,.$$

For $\vartheta^{\langle 1\times 3\rangle}_{(1,3)}$ it holds that $\hat{\boldsymbol{\omega}}_1 * \boldsymbol{R}(\vartheta^{\langle 1\times 3\rangle}_{(1,3)}, \hat{\boldsymbol{\omega}}_{\times 13}) \cdot \hat{\boldsymbol{\omega}}_3 = 1$, by definition. Assume (wlog) that $\hat{\boldsymbol{\omega}}_1$ and $\hat{\boldsymbol{\omega}}_3$ lie in the same half space with respect to $\hat{\boldsymbol{\omega}}_2$, so that $\hat{\boldsymbol{\omega}}_1 * \hat{\boldsymbol{\omega}}_2 > 0$ and $\hat{\boldsymbol{\omega}}_3 * \hat{\boldsymbol{\omega}}_2 > 0$ and thus $\hat{\boldsymbol{\omega}}_1 * \hat{\boldsymbol{\omega}}^{\boxtimes}_2 \cdot \hat{\boldsymbol{\omega}}_3 = \|\boldsymbol{\omega}_{1\|2}\| \cdot \|\boldsymbol{\omega}_{3\|2}\|$. Then, the inequality

$$1 - \|\boldsymbol{\omega}_{1\|2}\| \cdot \|\boldsymbol{\omega}_{3\|2}\| > \|\boldsymbol{\omega}_{1\perp 2}\| \cdot \|\boldsymbol{\omega}_{1\perp 2}\| \,.$$

follows from the strict Cauchy-Schwarz inequality $\boldsymbol{x} * \boldsymbol{y} < \|\boldsymbol{x}\| \cdot \|\boldsymbol{y}\|$ for $\boldsymbol{x} := (\|\boldsymbol{\omega}_{1\|2}\|, \|\boldsymbol{\omega}_{1\perp 2}\|)^T$ and $\boldsymbol{y} := (\|\boldsymbol{\omega}_{3\|2}\|, \|\boldsymbol{\omega}_{3\perp 2}\|)^T$ with $|\boldsymbol{x} * \boldsymbol{y}| < 1$ (because of genericity $\vartheta_{[1|2]} \neq \vartheta_{[2|3]}$). Therefore, the point $\vartheta^{\langle 1\times 3\rangle}_{(1,3)} \cdot \hat{\boldsymbol{\omega}}_{\times 13}$ lies in the *interior* of $\mathcal{T}^{[+]}$. With a similar argumentation, one shows that the point $\vartheta^{\langle 1\times 3\rangle[-1]}_{(1,3)} \cdot \hat{\boldsymbol{\omega}}_{\times 13}$ lies in the *interior* of $\mathcal{T}^{[-]}$. Therefore, $\hat{\boldsymbol{\omega}}_{\times 13}$ is a secant line of $\mathcal{T}^{[+]}$ and $\mathcal{T}^{[-]}$. The intersection of the secant line $[\hat{\boldsymbol{\omega}}_{\times 13}]$ with the toroids $\mathcal{T}^{[+]}$ and $\mathcal{T}^{[-]}$ are computed by solving the following two inverted problems.

Problem 3 (Inverse Decompositions)**.** *Given the axes of the primal Problem 1, and singular rotations $\boldsymbol{R}^{[+]}_2$ and $\boldsymbol{R}^{[-]}_2$ (as introduced in Theorem 2), (i) find angles $\phi_1, \phi_{\times 13}, \phi_3$ such that*

$$\boldsymbol{R}^{[+]}_2 \stackrel{!}{=} \boldsymbol{R}(\phi_1; -\hat{\boldsymbol{\omega}}_1) \cdot \boldsymbol{R}(\phi_{\times 13}; \hat{\boldsymbol{\omega}}_{\times 13}) \cdot \boldsymbol{R}(\phi_3, -\hat{\boldsymbol{\omega}}_3) \,,$$

and (ii) find angles $\phi_1, \phi_{\times 13}, \phi_3$ such that

$$\boldsymbol{R}^{[-]}_2 \stackrel{!}{=} \boldsymbol{R}(\phi_1; -\hat{\boldsymbol{\omega}}_1) \cdot \boldsymbol{R}(\phi_{\times 13}; \hat{\boldsymbol{\omega}}_{\times 13}) \cdot \boldsymbol{R}(\phi_3, -\hat{\boldsymbol{\omega}}_3) \,.$$

Each of the two inverse problems are variants of Problem 1 with perpendicular axes. Thus, simple variants of the computations of Section 3.1 are conducted in the following. As before (Equation 11), the solutions of each of the inverse problems have the form $\varphi_{1,2} = \operatorname{atan}_2(b, a) \pm \operatorname{atan}_2(d, c)$ for which convenient definitions are introduced with

$$\phi^{[+]_0}_{\times 13} := \operatorname{atan}^{\star}_2 \frac{\overline{b}}{\overline{a}} \qquad \phi^{[-]_0}_{\times 13} := \left(\phi^{[+]_0}_{\times 13}\right)^{[-1]}$$

$$\phi^{[+]_\Delta}_{\times 13} := \operatorname{atan}^{\star}_2 \frac{\overline{d}^{[+]}}{\overline{c}^{[+]}} \qquad \phi^{[-]_\Delta}_{\times 13} := \operatorname{atan}^{\star}_2 \frac{\overline{d}^{[-]}}{\overline{c}^{[-]}} \,.$$

These are simplified by means of the equations in Section 2.2. First, $\overline{a}$ is determined by Equation 5 as

$$\overline{a} = \hat{\boldsymbol{\omega}}_1 * (-(\hat{\boldsymbol{\omega}}^{\otimes}_{\times 13})^2) \cdot \hat{\boldsymbol{\omega}}_3 = \cos \vartheta^{\langle 1\times 3\rangle}_{(1,3)} \,.$$

Second, $\overline{b}$ is determined by Equation 4 as

$$\overline{b} = \hat{\boldsymbol{\omega}}_1 * \hat{\boldsymbol{\omega}}^{\otimes}_{\times 13} \cdot \hat{\boldsymbol{\omega}}_3 = -\sin \vartheta^{\langle 1\times 3\rangle}_{(1,3)} \,.$$

Combining these two results, $\operatorname{atan}_2(\overline{b}, \overline{a})$ is simplified with Equation A.1 and Equation A.2 to

$$\phi^{[+]_0}_{\times 13} = \operatorname{atan}^{\star}_2 \frac{\overline{b}}{\overline{a}} = \operatorname{atan}^{\star}_2 \frac{-\sin \vartheta^{\langle 1\times 3\rangle}_{(1,3)}}{\cos \vartheta^{\langle 1\times 3\rangle}_{(1,3)}} = \vartheta^{\langle 1\times 3\rangle}_{(1,3)} = \operatorname{acos}^{\star}_3\left(\hat{\boldsymbol{\omega}}_1, \hat{\boldsymbol{\omega}}_3; \hat{\boldsymbol{\omega}}_3 \times \hat{\boldsymbol{\omega}}_1\right) \tag{13}$$

Via the sequential orthogonality $\hat{\boldsymbol{\omega}}_1 \perp \hat{\boldsymbol{\omega}}_{\times 13} \perp \hat{\boldsymbol{\omega}}_3$, thus $\hat{\boldsymbol{\omega}}_1 * \hat{\boldsymbol{\omega}}^{\boxtimes}_{\times 13} \cdot \hat{\boldsymbol{\omega}}_3 = 0$, the parameter $\overline{c}^{[+]}$ is simplified to

$$\overline{c}^{[+]} = \hat{\boldsymbol{\omega}}_1 * (\boldsymbol{R}^{[+]}_2 - \hat{\boldsymbol{\omega}}^{\boxtimes}_{\times 13}) \cdot \hat{\boldsymbol{\omega}}_3 = \hat{\boldsymbol{\omega}}_1 * \boldsymbol{R}^{[+]}_2 \cdot \hat{\boldsymbol{\omega}}_3 \,.$$

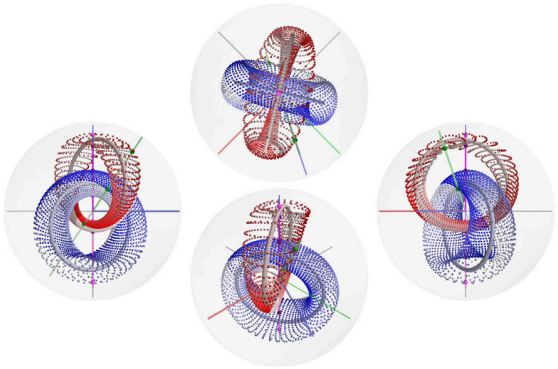

FIGURE 7. Toroids $\mathcal{T}^{[+]}$ and $\mathcal{T}^{[-]}$ for a generic constellation of rotation axes (b), $\hat{\boldsymbol{\omega}}_1 = (1,0,0)^T$ (red), $\hat{\boldsymbol{\omega}}_2 = (1,2,3)^{\odot T}$ (green), $\hat{\boldsymbol{\omega}}_3 = (1,2,0)^{\odot T}$ (blue), with symmetry axis $\hat{\boldsymbol{\omega}}_{\times 13} = (0,0,1)^T$ (purple), and circles $\mathcal{C}^{[+]}$, $\mathcal{C}^{[-]}$. The toroids are sampled with density 10°.

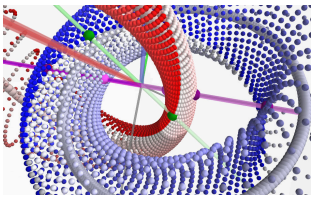

FIGURE 8. A close up view of Figure 7, with tangent $\hat{\boldsymbol{\omega}}_2$ (green), secant $\hat{\boldsymbol{\omega}}_{\times 13}$ (purple), and intersection points.

Analogously, the parameter $\bar{c}^{[-]}$ is simplified to

$$\bar{c}^{[-]} = \hat{\boldsymbol{\omega}}_1 * (\boldsymbol{R}_2^{[-]} - \hat{\boldsymbol{\omega}}_{\times 13}^{\boxtimes}) \cdot \hat{\boldsymbol{\omega}}_3 = \hat{\boldsymbol{\omega}}_1 * \boldsymbol{R}_2^{[-]} \cdot \hat{\boldsymbol{\omega}}_3 \,.$$

Using the quadratic identity $\bar{a}^2 + \bar{b}^2 = 1$, one derives for $\bar{d}^{[+]}$ and $\bar{d}^{[-]}$ (with $\bar{d}^{[\cdot]} = \sqrt{\bar{a}^2 + \bar{b}^2 - (\bar{c}^{[\cdot]})^2}$) that

$$\bar{d}^{[+]} = \sqrt{1 - (\bar{c}^{[+]})^2} \qquad\qquad \bar{d}^{[-]} = \sqrt{1 - (\bar{c}^{[-]})^2} \,.$$

Combining these two results the expression $\operatorname{atan}_2(\bar{d}^{[+]}, \bar{c}^{[+]})$ for toroid $\mathcal{T}^{[+]}$ is reduced, with $|\bar{\gamma}^{[+]}| := \operatorname{acos}(\bar{c}^{[+]}) = \operatorname{acos}(\hat{\boldsymbol{\omega}}_1 * \boldsymbol{R}_2^{[+]} \cdot \hat{\boldsymbol{\omega}}_3)$, similarly to Equation 13, with Equation A.4 to

$$\phi_{\times 13}^{[+]\Delta} = \operatorname{atan}_2^\star \frac{\bar{d}^{[+]}}{\bar{c}^{[+]}} = \operatorname{atan}_2^\star \frac{|\sin \bar{\gamma}^{[+]}|}{\cos \bar{\gamma}^{[+]}} = |\bar{\gamma}^{[+]}| = \operatorname{acos}(\hat{\boldsymbol{\omega}}_1 * \boldsymbol{R}_2^{[+]} \cdot \hat{\boldsymbol{\omega}}_3) \,. \tag{14}$$

Combining Equation 13 and Equation 14, one yields

$$\phi_{\times 13}^{[+]+}, \phi_{\times 13}^{[+]-} = \phi_{\times 13}^{[+]0} \pm \phi_{\times 13}^{[+]\Delta} = \vartheta_{(1,3)}^{\langle 1\times 3\rangle} \pm |\bar{\gamma}^{[+]}| \tag{15}$$

for toroid $\mathcal{T}^{[+]}$. Analogously, with $|\bar{\gamma}^{[-]}| := \operatorname{acos}(\bar{c}^{[-]}) = \operatorname{acos}(\hat{\boldsymbol{\omega}}_1 * \boldsymbol{R}_2^{[-]} \cdot \hat{\boldsymbol{\omega}}_3)$, the equations

$$\phi_{\times 13}^{[-]+}, \phi_{\times 13}^{[-]-} = \phi_{\times 13}^{[-]0} \pm \phi_{\times 13}^{[-]\Delta} = \vartheta_{(1,3)}^{\langle 1\times 3\rangle} \pm |\bar{\gamma}^{[-]}| \tag{16}$$

are derived for toroid $\mathcal{T}^{[-]}$. □

With the next theorem, the mutual orthogonality of the central axes and central circles of the toroids is shown.

Theorem 3 (Orthogonal Interlacing)**.** *Given an instance of Problem 2, the toroids $\mathcal{T}^{[+]}$ and $\mathcal{T}^{[-]}$ as defined in Theorem 2 are orthogonally interlaced. In particular, the following holds:*

1. Both toroids contain central circles $\mathcal{C}^{[+]}$ and $\mathcal{C}^{[-]}$ defined for $\phi_1 \in (-\pi, \pi]$, $\phi_3 \in (-\pi, \pi]$ as

$$\mathcal{C}^{[+]} := \left\{ v^\star(\boldsymbol{R}) \in \mathcal{B}^3 \;\middle|\; \boldsymbol{R} = \boldsymbol{R}(\phi_1; \hat{\boldsymbol{\omega}}_1) \cdot \boldsymbol{R}_m^{[+]} \right\}$$
$$\mathcal{C}^{[-]} := \left\{ v^\star(\boldsymbol{R}) \in \mathcal{B}^3 \;\middle|\; \boldsymbol{R} = \boldsymbol{R}_m^{[-]} \cdot \boldsymbol{R}(\phi_3, \hat{\boldsymbol{\omega}}_3) \right\} .$$

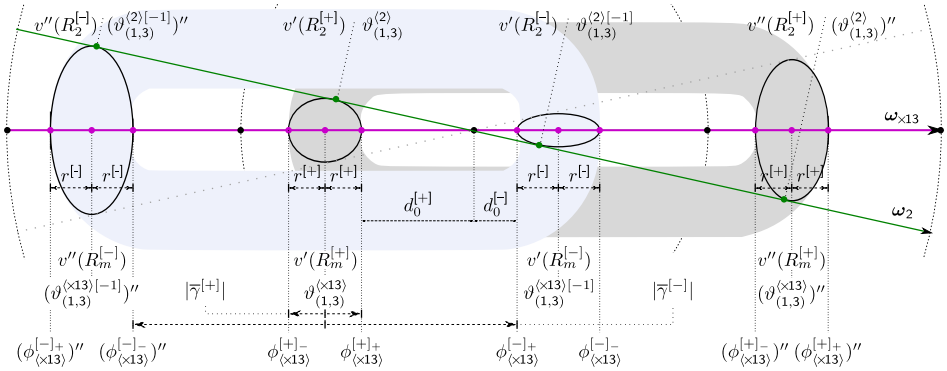

FIGURE 9. Scheme of the toroids $\mathcal{T}^{[+]}$ (gray) and $\mathcal{T}^{[-]}$ (blue) with tangent line $\hat{\boldsymbol{\omega}}_2$ (green), symmtry axis $\hat{\boldsymbol{\omega}}_{\times 13}$ (purple) and further geometric features: points in the inner shelf of the unit ball named as $\boldsymbol{v}'(.)$, in the outer shelf as $\boldsymbol{v}''(.)$, boundary points of $\mathcal{T}^{[+]}$ and $\mathcal{T}^{[-]}$ with $\hat{\boldsymbol{\omega}}_2$ at values related to $\vartheta^{\langle 2\rangle}_{(1,3)}$, intersections of the central circles $\mathcal{C}^{[+]}$ and $\mathcal{C}^{[-]}$ with $\hat{\boldsymbol{\omega}}_{\times 13}$ at values related to $\vartheta^{\langle 1\times 3\rangle}_{(1,3)}$, intersections of $\mathcal{T}^{[+]}$ and $\mathcal{T}^{[-]}$ with $\hat{\boldsymbol{\omega}}_{\times 13}$ given via $\overline{\gamma}^{[+]}$ and $\overline{\gamma}^{[-]}$, or via $r^{[+]}$ and $r^{[-]}$, with respect to the circles.

2. *With* $\hat{\boldsymbol{\omega}}_{\hat{\times}(113)} := (\hat{\boldsymbol{\omega}}_1 \times (\hat{\boldsymbol{\omega}}_1 \times \hat{\boldsymbol{\omega}}_3))^{\circledcirc}$ *and* $\hat{\boldsymbol{\omega}}_{\hat{\times}(133)} := ((\hat{\boldsymbol{\omega}}_1 \times \hat{\boldsymbol{\omega}}_3) \times \hat{\boldsymbol{\omega}}_3)^{\circledcirc}$ *(Section 2.1), the central axes of* $\mathcal{T}^{[+]}$ *and* $\mathcal{T}^{[-]}$ *have the directions*

$$\hat{\boldsymbol{\omega}}^{[+]} := (\hat{\boldsymbol{\omega}}_{\hat{\times}(113)} - \hat{\boldsymbol{\omega}}_{\hat{\times}(133)})^{\circledcirc}$$
$$\hat{\boldsymbol{\omega}}^{[-]} := (\hat{\boldsymbol{\omega}}_{\hat{\times}(113)} + \hat{\boldsymbol{\omega}}_{\hat{\times}(133)})^{\circledcirc},$$

which are mutually orthogonal, $\hat{\boldsymbol{\omega}}^{[+]} \perp \hat{\boldsymbol{\omega}}^{[-]}$.

For proving Theorem 3, the formula by *Baker-Campbell-Hausdorff* (BCH) formula is used.

Definition 5 (BCH Formula)**.** Given two rotation vectors, $\phi_{\mathsf{A}} \cdot \hat{\boldsymbol{\omega}}_{\mathsf{A}}$, of a rotation $\boldsymbol{R}_{\mathsf{A}}$, and $\phi_{\mathsf{B}} \cdot \hat{\boldsymbol{\omega}}_{\mathsf{B}}$, of a rotation $\boldsymbol{R}_{\mathsf{B}}$, the rotation vector $\phi_{\mathsf{A},\mathsf{B}} \cdot \hat{\boldsymbol{\omega}}_{\mathsf{A},\mathsf{B}}$ of the concatenated rotation $\boldsymbol{R}_{\mathsf{A},\mathsf{B}} = \boldsymbol{R}_{\mathsf{A}} \cdot \boldsymbol{R}_{\mathsf{B}}$ is computed with $\boldsymbol{\omega}_{\times\mathsf{AB}} := \hat{\boldsymbol{\omega}}_{\mathsf{A}} \times \hat{\boldsymbol{\omega}}_{\mathsf{B}}$ as

$$\phi_{\mathsf{A},\mathsf{B}} \cdot \hat{\boldsymbol{\omega}}_{\mathsf{A},\mathsf{B}} = \mathtt{BCH}\big(\phi_{\mathsf{A}} \cdot \hat{\boldsymbol{\omega}}_{\mathsf{A}}, \phi_{\mathsf{B}} \cdot \hat{\boldsymbol{\omega}}_{\mathsf{B}}\big) = \phi_{\mathsf{A},\mathsf{B}} \cdot \big(a \cdot \hat{\boldsymbol{\omega}}_{\mathsf{A}} + b \cdot \hat{\boldsymbol{\omega}}_{\mathsf{B}} + c \cdot \boldsymbol{\omega}_{\times\mathsf{AB}}\big),$$

where the rotation angle $\phi_{\mathsf{A},\mathsf{B}}$ is determined via

$$\cos\frac{\phi_{\mathsf{A},\mathsf{B}}}{2} = \cos\frac{\phi_{\mathsf{A}}}{2} \cdot \cos\frac{\phi_{\mathsf{B}}}{2} - \sin\frac{\phi_{\mathsf{A}}}{2} \cdot \sin\frac{\phi_{\mathsf{B}}}{2} \cdot (\hat{\boldsymbol{\omega}}_{\mathsf{A}} * \hat{\boldsymbol{\omega}}_{\mathsf{B}}),$$

and the coefficients a, b, and c are determined via the three equations

$$a \cdot \sin\frac{\phi_{\mathsf{A},\mathsf{B}}}{2} = \sin\frac{\phi_{\mathsf{A}}}{2} \cdot \cos\frac{\phi_{\mathsf{B}}}{2} \qquad b \cdot \sin\frac{\phi_{\mathsf{A},\mathsf{B}}}{2} = \cos\frac{\phi_{\mathsf{A}}}{2} \cdot \sin\frac{\phi_{\mathsf{B}}}{2}$$
$$c \cdot \sin\frac{\phi_{\mathsf{A},\mathsf{B}}}{2} = \sin\frac{\phi_{\mathsf{A}}}{2} \cdot \sin\frac{\phi_{\mathsf{B}}}{2}.$$

The BCH formula is derived, for example, in [21], a proof can be found in [24].

Proof. 1. Central Circles: The definition of the cirlces $\mathcal{C}^{[+]}$ and $\mathcal{C}^{[-]}$ via $\phi^{[+]0}_{\times 13}$ and $\phi^{[-]0}_{\times 13}$ lying in the middle of the intersections of axis $\hat{\boldsymbol{\omega}}_{\times 13}$ with $\mathcal{T}^{[+]}$ and $\mathcal{T}^{[-]}$ (see proof of Theorem 3) implies their centrality.
2. Orthogonality. The two axes $\hat{\boldsymbol{\omega}}^{[+]} = (\hat{\boldsymbol{\omega}}_{\hat{\times}(113)} - \hat{\boldsymbol{\omega}}_{\hat{\times}(133)})^{\circledcirc}$ and $\hat{\boldsymbol{\omega}}^{[-]} = (\hat{\boldsymbol{\omega}}_{\hat{\times}(113)} + \hat{\boldsymbol{\omega}}_{\hat{\times}(133)})^{\circledcirc}$ are mutual perpendicular, $\hat{\boldsymbol{\omega}}^{[+]} \perp \hat{\boldsymbol{\omega}}^{[-]}$, since it holds that $\hat{\boldsymbol{\omega}}^{[+]} * \hat{\boldsymbol{\omega}}^{[-]} = (\hat{\boldsymbol{\omega}}_{\hat{\times}(113)})^2 - (\hat{\boldsymbol{\omega}}_{\hat{\times}(133)})^2 = 0$ with $\|\hat{\boldsymbol{\omega}}_{\hat{\times}(113)}\| = \|\hat{\boldsymbol{\omega}}_{\hat{\times}(133)}\| = 1$. To derive the mutual orthogonality of the toroids $\mathcal{T}^{[+]}$ and $\mathcal{T}^{[-]}$, it is therefore sufficient to account for

$$\mathcal{C}^{[+]} \perp \hat{\boldsymbol{\omega}}^{[+]} \qquad\qquad \mathcal{C}^{[-]} \perp \hat{\boldsymbol{\omega}}^{[-]}, \tag{17}$$

of the central circles $\mathcal{C}^{[+]}$ and $\mathcal{C}^{[-]}$. Eq. 17 is shown by applying the BCH formula to arbitrary rotations

$$\boldsymbol{R}^{[+]}_{133}(\phi_1) = \boldsymbol{R}_1(\phi_1) \cdot \boldsymbol{R}^{[+]}_m \qquad\qquad \boldsymbol{R}^{[-]}_{133}(\phi_3) = \boldsymbol{R}^{[-]}_m \cdot \boldsymbol{R}_3(\phi_3). \tag{18}$$

Features	Related Term	Toroid $\mathcal{T}^{[+]}$	Toroid $\mathcal{T}^{[-]}$	Convolution
Tangentials $\phi_2^{[.]}$	$\mathrm{atan}_2(b,a)$	$\phi_2^{[+]} = \vartheta_{(1,3)}^{\langle 2\rangle}$	$\phi_2^{[-]} = (\vartheta_{(1,3)}^{\langle 2\rangle})^{[-1]}$	$\lvert\phi_2^{[+]}\rvert + \lvert\phi_2^{[-]}\rvert = \pi$
Circle points $m^{[.]}$	$\mathrm{atan}_2(\overline{b},\overline{a})$	$m^{[+]} = \vartheta_{(1,3)}^{\langle\times 13\rangle}$	$m^{[-]} = (\vartheta_{(1,3)}^{\langle\times 13\rangle})^{[-1]}$	$\lvert m^{[+]}\rvert + \lvert m^{[-]}\rvert = \pi$
Intersections $\phi_{\times 13}^{[.]\pm}$	$\mathrm{atan}_2^\star\frac{\overline{b}}{a}\cdots\pm\mathrm{atan}_2^\star\frac{\overline{d}^{[.]}}{\overline{c}^{[.]}}\cdots$	$\phi_{\times 13}^{[-]+} \quad \phi_{\times 13}^{[+]-}$	$\phi_{\times 13}^{[-]+} \quad \phi_{\times 13}^{[-]-}$	$\left\lvert\phi_{\times 13}^{[.]+} - \phi_{\times 13}^{[.]-}\right\rvert = 2\cdot r^{[.]}$
Radii $r^{[.]}$	$\mathrm{atan}_2(\overline{d}^{[.]},\overline{c}^{[.]})$	$r^{[+]} = \lvert\vartheta_{\lvert 1\rvert 2]} - \vartheta_{\lvert 2\rvert 3]}\rvert$	$r^{[-]} = \left\lvert\pi - \lvert\vartheta_{\lvert 1\rvert 2]} + \vartheta_{\lvert 2\rvert 3]}\rvert\right\rvert$	$r^{[+]} + r^{[-]} = \Delta^{(0)}$
Distances $d^{[.]}$	$m^{[.]} - r^{[.]}$	$d^{[+]} = \lvert m^{[+]}\rvert - r^{[+]}$	$d^{[-]} = \lvert m^{[-]}\rvert - r^{[-]}$	$d^{[+]} + d^{[-]} = \Delta^{(2)}$
				$\Delta^{(0)} + \Delta^{(2)} = \pi$

TABLE 1. Overview of characteristic geometric features of the toroids $\mathcal{T}^{[+]}$ and $\mathcal{T}^{[-]}$: boundary points with the tangential $\hat{\boldsymbol{\omega}}_2$ at angles $\phi_2^{[.]}$ and essential points and sizes along the symmetry axis $\hat{\boldsymbol{\omega}}_{\times 13}$.

of the circles $\mathcal{C}^{[+]}$ and $\mathcal{C}^{[-]}$. Since the relation between a rotation vector and the angle-axis representation of a rotation is 'bi-ambiguous', because of $\phi\cdot\hat{\boldsymbol{\omega}} = \overline{\phi}\cdot(-\hat{\boldsymbol{\omega}})$, the signs of angles and axes have to treated cautiously, compare Appendix B. In particular, since the signs of the rotation angles of $\boldsymbol{R}_m^{[+]}$ and $\boldsymbol{R}_m^{[-]}$ in Equation 18 differ, $\mathrm{sgn}(\vartheta_{(1,3)}^{\langle 1\times 3\rangle}) \neq \mathrm{sgn}\big((\vartheta_{(1,3)}^{\langle 1\times 3\rangle})^{[-1]}\big)$, a case distinction has to be applied to ensure that the orientations of $\hat{\boldsymbol{\omega}}_{\times 13}$ are not swapped when the BCH formula is applied for elements of $\mathcal{C}^{[+]}$ and $\mathcal{C}^{[-]}$. For the case $\vartheta_{(1,3)}^{\langle 1\times 3\rangle} < 0$, it holds that $\vartheta_{\lvert 1,3\rvert} = -\vartheta_{(1,3)}^{\langle 1\times 3\rangle}$ and, in particular, that the two angles $-\vartheta_{\lvert 1,3\rvert}$ and $\pi - \vartheta_{\lvert 1,3\rvert}$ are elements of the interval $[0,\pi]$. With respect to these angles, $\boldsymbol{R}_m^{[+]}$ and $\boldsymbol{R}_m^{[-]}$ are expressed as

$$\begin{aligned}\boldsymbol{R}_m^{[+]} &= \boldsymbol{R}(-\vartheta_{\lvert 1,3\rvert};\hat{\boldsymbol{\omega}}_{\times 13}) = \boldsymbol{R}(\vartheta_{(1,3)}^{\langle 1\times 3\rangle};\hat{\boldsymbol{\omega}}_{\times 13})\\ \boldsymbol{R}_m^{[-]} &= \boldsymbol{R}(\pi - \vartheta_{\lvert 1,3\rvert};\hat{\boldsymbol{\omega}}_{\times 13}) = \boldsymbol{R}((\vartheta_{(1,3)}^{\langle 1\times 3\rangle})^{[-1]};\hat{\boldsymbol{\omega}}_{\times 13})\,.\end{aligned}$$

For the second case with $\vartheta_{(1,3)}^{\langle 1\times 3\rangle} > 0$ one defines $\boldsymbol{R}(\vartheta_{\lvert 1,3\rvert};\hat{\boldsymbol{\omega}}_{\times 13}) = \boldsymbol{R}_m^{[+]}$ and $\boldsymbol{R}(\pi - \vartheta_{\lvert 1,3\rvert};\hat{\boldsymbol{\omega}}_{\times 13}) = \boldsymbol{R}_m^{[-]}$ and the proof works analogously. Applying the BCH formula to a rotation in $\mathcal{C}^{[+]}$ (Equation 18) results in

$$\phi_{113}\cdot\hat{\boldsymbol{\omega}}_{113}^{[+]} = \mathtt{BCH}\Big(\phi_1\cdot\hat{\boldsymbol{\omega}}_1,\, -\vartheta_{\lvert 1,3\rvert}\cdot\hat{\boldsymbol{\omega}}_{\times 13}\Big) = \frac{\phi_{113}}{\sin\frac{\phi_{113}}{2}}\cdot\Big(a^{[+]}\cdot\hat{\boldsymbol{\omega}}_1 + b^{[+]}\cdot\hat{\boldsymbol{\omega}}_{\times 13} + c^{[+]}\cdot\hat{\boldsymbol{\omega}}_{\hat{\times}(113)}\Big).$$

Applying the formula to an element of $\mathcal{C}^{[-]}$ results in

$$\phi_{133}\cdot\hat{\boldsymbol{\omega}}_{133}^{[-]} = \mathtt{BCH}\Big(\vartheta_{\lvert 1,3\rvert}\cdot\hat{\boldsymbol{\omega}}_{\times 13},\, \phi_3\cdot\hat{\boldsymbol{\omega}}_3\Big) = \frac{\phi_{133}}{\sin\frac{\phi_{133}}{2}}\cdot\Big(a^{[-]}\cdot\hat{\boldsymbol{\omega}}_{\times 13} + b^{[-]}\cdot\hat{\boldsymbol{\omega}}_3 + c^{[-]}\cdot\hat{\boldsymbol{\omega}}_{\hat{\times}(133)}\Big)\,.$$

The direction of a rotation vector in $\mathcal{C}^{[+]}$ is determined by the coefficients $a^{[+]}$, $b^{[+]}$, and $c^{[+]}$. By omitting constant factors and using the abbrevations $s_1 := \sin\frac{\phi_1}{2}$ and $c_1 := \cos\frac{\phi_1}{2}$, their ratio is denoted by

$$\begin{aligned}\big[a^{[+]} : b^{[+]} : c^{[+]}\big] &= \Big[s_1\cdot\cos\frac{-\vartheta_{\lvert 1,3\rvert}}{2} : c_1\cdot\sin\frac{-\vartheta_{\lvert 1,3\rvert}}{2} : s_1\cdot\sin\frac{-\vartheta_{\lvert 1,3\rvert}}{2}\Big]\\ &= \Big[s_1\cdot\cos\frac{\vartheta_{\lvert 1,3\rvert}}{2} : -c_1\cdot\sin\frac{\vartheta_{\lvert 1,3\rvert}}{2} : -s_1\cdot\sin\frac{\vartheta_{\lvert 1,3\rvert}}{2}\Big]\,.\end{aligned}$$

Similarly, the ratio of the coefficients $a^{[-]}$, $b^{[-]}$, and $c^{[-]}$ determining a rotation vector in $\mathcal{C}^{[-]}$ is written, with $s_3 := \sin\frac{\phi_3}{2}$ and $c_3 := \cos\frac{\phi_3}{2}$, as

$$\begin{aligned}\big[a^{[-]} : b^{[-]} : c^{[-]}\big] &= \Big[s_3\cdot\cos\frac{\phi_3}{2} : c_3\cdot\sin\frac{\phi_3}{2} : s_3\cdot\sin\frac{\phi_3}{2}\Big]\\ &= \Big[c_3\cdot\cos\frac{\phi_3}{2} : s_3\cdot\sin\frac{\phi_3}{2} : c_3\cdot\sin\frac{\phi_3}{2}\Big]\,.\end{aligned}$$

Using the identities

$$\begin{aligned}\hat{\boldsymbol{\omega}}_1 * (\hat{\boldsymbol{\omega}}_{\hat{\times}(113)} - \hat{\boldsymbol{\omega}}_{\hat{\times}(133)})^{\circledcirc} &= +\sin\frac{\vartheta_{\lvert 1,3\rvert}}{2}\\ \hat{\boldsymbol{\omega}}_{\hat{\times}(113)} * (\hat{\boldsymbol{\omega}}_{\hat{\times}(113)} - \hat{\boldsymbol{\omega}}_{\hat{\times}(133)})^{\circledcirc} &= +\cos\frac{\vartheta_{\lvert 1,3\rvert}}{2}\,,\end{aligned}$$

the scalar product of a rotation vector $\hat{\boldsymbol{\omega}}_{113}^{[+]}$ and the axis $\hat{\boldsymbol{\omega}}^{[+]}$ is evaluated to

$$\begin{aligned}\hat{\boldsymbol{\omega}}_{113}^{[+]} * \hat{\boldsymbol{\omega}}^{[+]} &= a^{[+]} \cdot \hat{\boldsymbol{\omega}}_1 * \hat{\boldsymbol{\omega}}^{[+]} + c^{[+]} \cdot \hat{\boldsymbol{\omega}}_{\hat{\times}(113)} * \hat{\boldsymbol{\omega}}^{[+]} \\ &= s_1 \cdot \big(\cos\tfrac{\vartheta_{|1,3|}}{2} \cdot \sin\tfrac{\vartheta_{|1,3|}}{2} - \sin\tfrac{\vartheta_{|1,3|}}{2} \cdot \cos\tfrac{\vartheta_{|1,3|}}{2}\big) = 0\,,\end{aligned}$$

thus $\hat{\boldsymbol{\omega}}_{113}^{[+]} \perp \hat{\boldsymbol{\omega}}^{[+]}$. Similarly, using the identities

$$\begin{aligned}\hat{\boldsymbol{\omega}}_3 * (\hat{\boldsymbol{\omega}}_{\hat{\times}(113)} + \hat{\boldsymbol{\omega}}_{\hat{\times}(133)})^{\circledcirc} &= -\cos\tfrac{\vartheta_{|1,3|}}{2} \\ \hat{\boldsymbol{\omega}}_{\hat{\times}(133)} * (\hat{\boldsymbol{\omega}}_{\hat{\times}(113)} + \hat{\boldsymbol{\omega}}_{\hat{\times}(133)})^{\circledcirc} &= +\sin\tfrac{\vartheta_{|1,3|}}{2}\,,\end{aligned}$$

the scalar product of a $\hat{\boldsymbol{\omega}}_{133}^{[-]}$ and $\hat{\boldsymbol{\omega}}^{[-]}$ is evaluated to

$$\begin{aligned}\hat{\boldsymbol{\omega}}_{133}^{[-]} * \hat{\boldsymbol{\omega}}^{[-]} &= (b^{[-]} \cdot \hat{\boldsymbol{\omega}}_3) * \hat{\boldsymbol{\omega}}^{[-]} + (c^{[-]} \cdot \hat{\boldsymbol{\omega}}_{\hat{\times}(133)}) * \hat{\boldsymbol{\omega}}^{[-]} \\ &= s_3 \cdot \big(\sin\tfrac{\vartheta_{|1,3|}}{2} \cdot (-\cos\tfrac{\vartheta_{|1,3|}}{2}) + \cos\tfrac{\vartheta_{|1,3|}}{2} \cdot \sin\tfrac{\vartheta_{|1,3|}}{2}\big) = 0,\end{aligned}$$

such that the orthogonality $\hat{\boldsymbol{\omega}}_{133}^{[-]} \perp \hat{\boldsymbol{\omega}}^{[-]}$ is derived. Therefore, for all $\boldsymbol{R}_{133}^{[+]}(\phi_1)$ and $\boldsymbol{R}_{133}^{[-]}(\phi_3)$ it holds that

$$\phi_{113} \cdot \hat{\boldsymbol{\omega}}_{113}^{[+]} \perp \hat{\boldsymbol{\omega}}^{[+]} \qquad\qquad \phi_{133} \cdot \hat{\boldsymbol{\omega}}_{133}^{[-]} \perp \hat{\boldsymbol{\omega}}^{[-]}$$

such that the feasibility of Equation 17 follows. □

With help of the mutual orthogonality of $\mathcal{C}^{[+]}$ and $\mathcal{C}^{[-]}$, and therefore of $\mathcal{T}^{[+]}$ and $\mathcal{T}^{[-]}$, one can further argue that (i) the toroids are *disjoint* (with an argument about maximum size of the cross sectional radii), (ii) they are *interlaced* (with an argument about the size of 2π of the central radii). The last of the three theorems defines the 'sizes' of the toroids by their cross sectional radii and their distances to identity.

Theorem 4 (Radii and Distances)**.** *Given an instance of Problem 2 and toroids $\mathcal{T}^{[+]}$ and $\mathcal{T}^{[-]}$ as defined in Theorem 2, following can be said about the radii and the distances of $\mathcal{T}^{[+]}$ and $\mathcal{T}^{[-]}$.*

1. The cross-sectional radii $r^{[-]}$ and $r^{[+]}$ of the toroids, measured along $\hat{\boldsymbol{\omega}}_{\times 13}$, are determined by

$$r^{[+]} = \big|\vartheta_{[1|2]} - \vartheta_{[2|3]}\big| \qquad\qquad r^{[-]} = \Big|\pi - \big|\vartheta_{[1|2]} + \vartheta_{[2|3]}\big|\Big|\,.$$

2. The distances of $\mathcal{T}^{[+]}$ and $\mathcal{T}^{[-]}$ to identity, $d^{[+]}$, $d^{[-]}$, are determined by

$$d^{[+]} = |m^{[+]}| - r^{[+]} \qquad\qquad d^{[-]} = |m^{[-]}| - r^{[-]}\,.$$

Proof. 1. Cross-Sectional Radii: With $|\overline{\gamma}^{[+]}|$ and $|\overline{\gamma}^{[-]}|$, previously defined as $|\overline{\gamma}^{[+]}| = |\mathrm{acos}(\hat{\boldsymbol{\omega}}_1 * \boldsymbol{R}_2^{[+]} \cdot \hat{\boldsymbol{\omega}}_3)|$ (Equation 14) and $|\overline{\gamma}^{[-]}| = |\mathrm{acos}(\hat{\boldsymbol{\omega}}_1 * \boldsymbol{R}_2^{[-]} \cdot \hat{\boldsymbol{\omega}}_3)|$, the radii are computed as $r^{[+]} = |\overline{\gamma}^{[+]}|$ and $r^{[-]} = |\pi - |\overline{\gamma}^{[-]}||$ (see Figure 9). Therefore, it remains to show

$$\begin{aligned}\big|\overline{\gamma}^{[+]}\big| &= \big|\vartheta_{[1|2]} - \vartheta_{[2|3]}\big| \\ \Big|\pi - \big|\overline{\gamma}^{[-]}\big|\Big| &= \Big|\pi - \big|\vartheta_{[1|2]} + \vartheta_{[2|3]}\big|\Big|\end{aligned} \tag{19}$$

Therefore, the 'left' expressions $\big|\overline{\gamma}^{[+]}\big| = \big|\mathrm{acos}(\hat{\boldsymbol{\omega}}_1 * \boldsymbol{R}_2^{[+]} \cdot \hat{\boldsymbol{\omega}}_3)\big|$ and $\big|\overline{\gamma}^{[-]}\big| = \big|\mathrm{acos}(\hat{\boldsymbol{\omega}}_1 * \boldsymbol{R}_2^{[-]} \cdot \hat{\boldsymbol{\omega}}_3)\big|$ are analyzed. As special versions of the Equation 8 in Section 2.2, for a rotation with the 'singular' angle $\vartheta_{(\boldsymbol{a},\boldsymbol{b})}^{\langle\hat{\boldsymbol{\omega}}\rangle}$ one yields the equation

$$\begin{aligned}\boldsymbol{a} * \boldsymbol{R}\big(\vartheta_{(\boldsymbol{a},\boldsymbol{b})}^{\langle\hat{\boldsymbol{\omega}}\rangle}, \hat{\boldsymbol{\omega}}\big) \cdot \boldsymbol{b} &= +\|\boldsymbol{a}_\Omega\| \cdot \|\boldsymbol{b}_\Omega\| + \|\boldsymbol{a}_{\hat{\boldsymbol{\omega}}}\| \cdot \|\boldsymbol{b}_{\hat{\boldsymbol{\omega}}}\| \\ &= +\sin\vartheta_{[\boldsymbol{a}|\hat{\boldsymbol{\omega}}]} \cdot \sin\vartheta_{[\boldsymbol{b}|\hat{\boldsymbol{\omega}}]} + \cos\vartheta_{[\boldsymbol{a}|\hat{\boldsymbol{\omega}}]} \cdot \cos\vartheta_{[\boldsymbol{b}|\hat{\boldsymbol{\omega}}]}\,,\end{aligned}$$

and for the 'singular' angle $\vartheta_{(\boldsymbol{a},-\boldsymbol{b})}^{\langle\hat{\boldsymbol{\omega}}\rangle}$ the equation

$$\begin{aligned}\boldsymbol{a} * \boldsymbol{R}\big(\vartheta_{(\boldsymbol{a},-\boldsymbol{b})}^{\langle\hat{\boldsymbol{\omega}}\rangle}, \hat{\boldsymbol{\omega}}\big) \cdot \boldsymbol{b} &= -\|\boldsymbol{a}_\Omega\| \cdot \|\boldsymbol{b}_\Omega\| + \|\boldsymbol{a}_{\hat{\boldsymbol{\omega}}}\| \cdot \|\boldsymbol{b}_{\hat{\boldsymbol{\omega}}}\| \\ &= -\sin\vartheta_{[\boldsymbol{a}|\hat{\boldsymbol{\omega}}]} \cdot \sin\vartheta_{[\boldsymbol{b}|\hat{\boldsymbol{\omega}}]} + \cos\vartheta_{[\boldsymbol{a}|\hat{\boldsymbol{\omega}}]} \cdot \cos\vartheta_{[\boldsymbol{b}|\hat{\boldsymbol{\omega}}]}\,.\end{aligned}$$

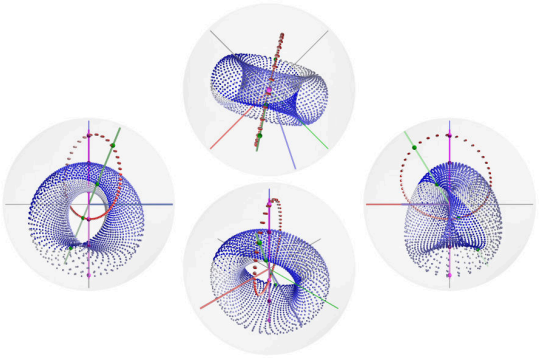

FIGURE 10. Toroids for a nearly symmetric constellation of rotation axes (c), with $\hat{\boldsymbol{\omega}}_1 = (1{,}0{,}0)^T$, $\hat{\boldsymbol{\omega}}_2 = \boldsymbol{R}\big(\frac{-30^\circ}{360^\circ}\cdot 2\pi, \boldsymbol{e}_z\big)\cdot(1{,}2{,}3)^{\odot T}$, $\hat{\boldsymbol{\omega}}_3 = (1{,}2{,}0)^{\odot T}$.

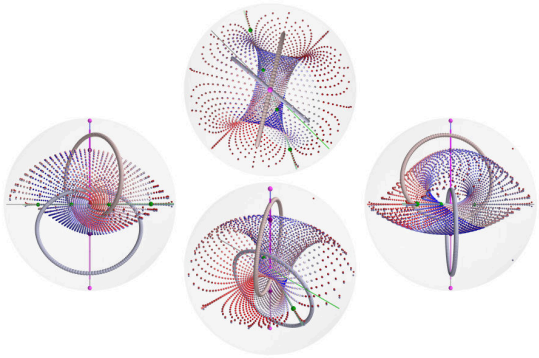

FIGURE 11. Toroids for a nearly coincident constellations of rotation axes (d), with $\hat{\boldsymbol{\omega}}_1 = (1{,}0{,}0)^T$, $\hat{\boldsymbol{\omega}}_2 = (1{,}2{,}\frac{1}{100})^{\odot T}$, and $\hat{\boldsymbol{\omega}}_3 = (1{,}2{,}0)^{\odot T}$.

		Minimal Line Angles			Non-Solvable Set			Two-Solvable Set		
Example	$\hat{\omega}_2$	$\vartheta_{[1\|2]}$	$\vartheta_{[2\|3]}$	$\vartheta_{[1\|3]}$	$r^{[+]}$	$r^{[-]}$	$\Delta^{(0)}$	$d^{[+]}$	$d^{[-]}$	$\Delta^{(2)}$
(a)	$(0,0,1)^T$	90°	90°	63.435°	0°	0°	0°	90°	90°	180°
(b)	$(1,2,3)^{\odot T}$	74.499°	53.300°	63.435°	21.198°	52.201°	73.399°	32.103°	74.498°	106.601°
(c)	$\boldsymbol{R}_z(\frac{-2\pi}{9})\cdot(1,2,3)^{\odot T}$	60.085°	58.832°	63.435°	1.253°	61.083°	62.336°	62.182°	55.482°	117.664°
(d)	$(1,2,\frac{1}{100})^{\odot T}$	63.435°	0.256°	63.435°	63.691°	116.309°	179.488°	0.256°	0.256°	0.512°

TABLE 2. Numerical comparison for examples (a), (b), (c), and (d); angle values are rounded to three digits.

Using these equations, auxilary variables $x_{123}^{[+]}$ and $x_{123}^{[-]}$ are defined as

$$x_{123}^{[+]} := \hat{\boldsymbol{\omega}}_1^T \cdot \boldsymbol{R}_2^{[+]} \cdot \hat{\boldsymbol{\omega}}_3 = +\sin\vartheta_{[1|2]} \cdot \sin\vartheta_{[2|3]} + \cos\vartheta_{[1|2]} \cdot \cos\vartheta_{[2|3]}\,, \tag{20}$$

$$x_{123}^{[-]} := \hat{\boldsymbol{\omega}}_1^T \cdot \boldsymbol{R}_2^{[-]} \cdot \hat{\boldsymbol{\omega}}_3 = -\sin\vartheta_{[1|2]} \cdot \sin\vartheta_{[2|3]} + \cos\vartheta_{[1|2]} \cdot \cos\vartheta_{[2|3]}\,. \tag{21}$$

With $x_{123}^{[+]}$ and $x_{123}^{[-]}$, the left expressions read as

$$\big|\overline{\gamma}^{[+]}\big| = \Big|\operatorname{acos}\big(x_{123}^{[+]}\big)\Big| \qquad\qquad \big|\overline{\gamma}^{[-]}\big| = \Big|\operatorname{acos}\big(x_{123}^{[-]}\big)\Big|\,.$$

For the expressions on the right, one examines for $\vartheta_{|1,2|}$ and for $\vartheta_{|2,3|}$, that by definition $0 \le \vartheta_{[i|j]} \le \frac{\pi}{2}$ hold, so that $\cos\vartheta_{[i|j]} \ge 0$ and $\sin\vartheta_{[i|j]} \ge 0$. Further, for $x = \cos\vartheta_{[1|2]}$ and $y = \cos\vartheta_{[2|3]}$, the inequalities $0 \le \operatorname{acos} x \pm \operatorname{acos} y \le \pi$ are fulfilled. Thus, the trigonometric identity

$$\operatorname{acos} x \pm \operatorname{acos} y = \operatorname{acos}\Big(x \cdot y \mp \sqrt{1-x^2}\cdot\sqrt{1-y^2}\Big)$$

can be applied for the sum and the difference of the angles $\vartheta_{|1,2|}$ and $\vartheta_{|2,3|}$ which yields

$$\begin{aligned}\vartheta_{|1,2|} \mp \vartheta_{|2,3|} &= \operatorname{acos}\big(\cos\vartheta_{[1|2]}\big) \mp \operatorname{acos}\big(\cos\vartheta_{[2|3]}\big) \\ &= \operatorname{acos}\big(\cos\vartheta_{[1|2]}\cdot\cos\vartheta_{[2|3]} \pm \sin\vartheta_{[1|2]}\cdot\sin\vartheta_{[2|3]}\big)\,.\end{aligned}$$

Using the definitions from Equation 20 and Equation 21 one has derived that

$$\big|\vartheta_{|1,2|} - \vartheta_{|2,3|}\big| = \Big|\operatorname{acos} x_{123}^{[+]}\Big| \qquad\qquad \big|\vartheta_{|1,2|} + \vartheta_{|2,3|}\big| = \Big|\operatorname{acos} x_{123}^{[-]}\Big|.$$

Thereby, the expression for $\mathrm{r}^{[+]}$ and for $\mathrm{r}^{[-]}$ in Equation 19 are derived.
2. Distances to Identity. The distances to identity follow immediately. □

By the terms for $r^{[+]}$ and $r^{[-]}$ in Equation 19 the *sizes* for the *unreachable fractions* of the workspace are measured by the *lack* of sequential orthgonality of the three axes, see also Section 3.3.

As a summary, the toroids' geometric features analyzed within the three theorems are displayed together in a schematic sketch in Figure 9. Their analytical relations are compiled in Table 1.

Set	**Rotation Axes**				
	1	2	3 sym.	3 gen.	3 ort.
Two-solvable	0	0	3	3	3
Non-solvable	3	3	0–3	3–3	0–0
Singular	1 Line	2 Line × Line	1∞2 Circle ∞ Toroid	2∞2 Toroid ∞ Toroid	1∞1 Circle ∞ Circle
Related Example		(d)	(c)	(b)	(a)

TABLE 3. Dimensions of solution sets with regard to the constellation of the axes; abbrevations *'sym.'*, *'gen.'*, and *'ort.'* short for *'sequential symmetric'*, *'generic'*, and *'sequential orthogonal'*.

3.3. **Examples.** Different types of constellations of the three axes $\hat{\boldsymbol{\omega}}_1$, $\hat{\boldsymbol{\omega}}_2$, and $\hat{\boldsymbol{\omega}}_3$ can be distinguished. They are named here as (a) 'sequential orthogonal', (b) 'generic', (c) 'sequential symmetric', and (d) 'coincident'. To compare these different cases, four examples are given which all feature $\hat{\boldsymbol{\omega}}_1 = (1,0,0)^T$ and $\hat{\boldsymbol{\omega}}_3 = (1,2,0)^{\odot T}$ and only differ in $\hat{\boldsymbol{\omega}}_2$. The influence of the pose of the second axis $\hat{\boldsymbol{\omega}}_2$ to the *radii* and the *distances* (Theorem 4) of the toroids is exemplified.
(a) A sequential-orthogonal case corresponds to a *Davenport constellation*. For the given $\hat{\boldsymbol{\omega}}_1$ and $\hat{\boldsymbol{\omega}}_3$, the second axis is $\hat{\boldsymbol{\omega}}_2 = \hat{\boldsymbol{\omega}}_1 \times \hat{\boldsymbol{\omega}}_3 = (0,0,1)^T$. The radii $\mathrm{r}^{[+]}$ and $\mathrm{r}^{[-]}$ both equal zero, the toroids are 'shrinked' to circles. (b) The generic case is assumed in the analysis before. An example is given with $\hat{\boldsymbol{\omega}}_2 = (1,2,3)^{\odot T}$. The toroids $\mathcal{T}^{[+]}$ and $\mathcal{T}^{[-]}$ are depicted in Figure 7 and Figure 8. The radii $\mathrm{r}^{[+]}$ and $\mathrm{r}^{[-]}$ are both greater zero. (c) An example for a case close to 'sequential symmetry' is given by $\hat{\boldsymbol{\omega}}_2 = \boldsymbol{R}\left(\frac{-30^\circ}{360^\circ} \cdot 2\pi, \boldsymbol{e}_z\right) \cdot (1,2,3)^{\odot T}$. The toroids $\mathcal{T}^{[+]}$ and $\mathcal{T}^{[-]}$ are depicted in Figure 10. The radius $\mathrm{r}^{[+]}$ is very small. (d) An example for a nearly coincident constellation is given by $\hat{\boldsymbol{\omega}}_2 = (1,2,\frac{1}{100})^{\odot T}$ for which the second axis nearly equals the third axis $\hat{\boldsymbol{\omega}}_3$. The toroids are illustrated in Figure 11. The radii $\mathrm{r}^{[+]}$ and $\mathrm{r}^{[-]}$ are so large that the toroids nearly fill the entire space of rotations.
In Table 2, the four examples are compared numerically with regard to the *minimal line angles* (Definition 7) between the rotation axes and to the *sizes* of the *constraint spaces* (non-solvable set) and the *sizes* of the *workspace interior* (two-solvable set) along $\hat{\boldsymbol{\omega}}_{\times 13}$ (see Theorem 4 and Table 1). Generalizing from the four examples, the dimensions of the workspace interior, the constraint space, and the singular set (one-solvable) are compared for different classes of axes' constellations in Table 3.

3.4. **Discussion.** The Theorems 2, 3, and 4 provide an explicit description of the boundary of the workspace of a spherical 3R chain with respect to the axes' constellation in 'global space', or, with respect to the *zero reference position* [8] of the rotation axes. Three cases occur: if a target orientation is located (i) *outside* both toroids, it is *reachable* with two configurations (two-solvable), (ii) on the *surface* of one toroid, it is on the *boundary* of the workspace and reachable with one configuration (one-solvable), (iii) in the *interior* of one toroid, it is *not reachable* (non-solvable).
Kinematic Synthesis. Such workspace description can be applied as a tool for solving the design problem of spherical mechanisms: If all reference target orientations are 'placed' inside the unit ball, the task is to orient rotation axes (according to external constraints) so that none of those is covered by the toroids. Due to the simple graphic representation, this can be done heuristically, or the description can be used to develop algorithmic approaches (comparable to [15], [10]) to determine an optimal axes' constellation. While *one* IK problem of a spherical 3R chain (Problem 1) can also be solved by computing the FK of *one* equivalent spherical four bar linkage (Section 1) [7], [25], [2], this does not hold for the generalized Problem 2. For the workspace problem, the features of the presented approach (parametric description of the workspace boundary with straight-forward visualization) complement existing techniques.
Control Problems. The derived workspace characterization can be used for following control problem: Given a spherical 3R chain and an infeasible target orientation $\boldsymbol{R}$, a feasible orientation close to $\boldsymbol{R}$ can be derived by the following method: (i) project the infeasible $\boldsymbol{R}$ onto the central circle, call the projection $\boldsymbol{R}_m$, (ii) build the ray from $\boldsymbol{R}_m$ through $\boldsymbol{R}$, (iii) the intersection of the ray with the toroid provides a feasible orientation nearby $\boldsymbol{R}$.
Modular Kinematics. Based on the algebra of dual unit quaternions, an algorithm to solve the IK of general 6R chains was developed [19], [12]. The 'kinematic image' of the workspace of a spherical

3R chain is a certain *3-manifold* in the representation of *(dual) unit quaternions*. For spherical axes, the *3-manifold* is contained in a *fixed 3-space* which can be specified via a system of four equations [19, Sec. 5.2.4]. With Theorems 2, 3, and 4, a description of the *fixed 3-manifold* is achieved in *unit ball representation* via the parametric specification of its toroidal boundary. Since the *unit ball representation* is equivalent to the *unit quaternion representation* (Appendix C), it allows to visualize basic, partial results of this algebraic approach. In the future, it will be interesting to analyze if and how the *unit ball representation* permits extensions to cope with boundaries on joint values, more than three rotation axes, and non-intersecting rotation axes (similar to the works based on level sets, see, for example [11]).

4. Conclusion

In this article, it was shown how the boundary of the workspace of three non-orthogonal rotation axes – the set of singular orientations – can be specified as two interlaced toroids. In three proven theorems, the toroids are specified with respect to the rotation axes and to the mutual angles between them. The results extend a recent theorem by Piovan and Bullo. The toroids' specification is based on a novel, primal-dual vectorial representation of rotations where the unit ball $\mathcal{B}^3(1)$ corresponds to a double cover of $SO(3)$. As explained, this rotation representation can be regarded equivalent to the quaternion representation and allows to visualize the structure of the workspace of three arbitrary, intersecting rotation axes due to its reduced dimension three. In addition to this representation, further 'geometric' tools (notation of directed angles, decomposition of rotation matrices) were developed to simplify and compactify the necessary notations. All tools are general and can find applications in context of other geometric computations.
In a discussion, potential applications and extensions of the novel workspace characterization were pointed out: For designing 3R mechanisms, the derived specification of the singular toroids provides the tools to reason about infeasible orientations. For control applications, the presented method can be used to determine realizable configurations close to infeasible target orientations. Extensions of the presented approach may provide insight into more general kinematic problems in future.

Acknowledgment. The author would like to thank Dr. Yohannes Kassahun and anonymous reviewers for their valuable comments on earlier versions of this document. The work presented in this article was funded by the German Ministry of Education and Research (BMBF) within the project Capio (Grant Number 01-IW-10001).

Contents

The appendix contains information about angles between vectors and lines in Appendix A. Issues about the orientation of angles and axes are discussed in Appendix B. The relation between unit ball representation and quaternions is outlined in Appendix C. An overview about the used notation is provided in Appendix D.

Appendix A. Undirected and Directed Angles

Undirected Angles for Vectors. Given two vectors $\boldsymbol{a}$ and $\boldsymbol{b}$, the *undirected angle* $|\measuredangle(\boldsymbol{a},\boldsymbol{b})| = |\measuredangle(\boldsymbol{b},\boldsymbol{a})| \in [0,\pi]$ between these is computed via the inverse tangent function as $|\measuredangle(\boldsymbol{a},\boldsymbol{b})| = \operatorname{atan}_2 \frac{\|\boldsymbol{a}\times\boldsymbol{b}\|}{\boldsymbol{a}*\boldsymbol{b}} \in [0,\pi]$.[6] In the next definition, a compact, symbolically equivalent[7] formulation is given via the inverse cosine function. The result is generalized for measuring the angle along an arbitrary line $[\hat{\boldsymbol{\omega}}]$.

Definition 6 (Undirected Angles)**.** Given two vectors $\boldsymbol{a}$ and $\boldsymbol{b}$, the (absolute) *undirected* angle $\big|\measuredangle(\boldsymbol{a},\boldsymbol{b})\big| \in [0,\pi]$ between $\boldsymbol{a}$ and $\boldsymbol{b}$ is defined as

$$\big|\measuredangle(\boldsymbol{a},\boldsymbol{b})\big| := \operatorname{acos}\big(\hat{\boldsymbol{a}} * \hat{\boldsymbol{b}}\big)$$

Given three vectors $\boldsymbol{a}$, $\boldsymbol{b}$, and $\hat{\boldsymbol{\omega}}$, the *relative undirected* angle $\big|\measuredangle_{[\hat{\boldsymbol{\omega}}]}(\boldsymbol{a},\boldsymbol{b})\big| \in [0,\pi]$ between $\boldsymbol{a}$ and $\boldsymbol{b}$ with respect to (undirected) line $[\hat{\boldsymbol{\omega}}]$ is defined as

$$\big|\measuredangle_{[\hat{\boldsymbol{\omega}}]}(\boldsymbol{a},\boldsymbol{b})\big| := \operatorname{acos}\big(\hat{\tau}_{\hat{\boldsymbol{\omega}}}(\boldsymbol{a}) * \hat{\tau}_{\hat{\boldsymbol{\omega}}}(\boldsymbol{b})\big)$$

As abbrevations, the notations $\vartheta_{|\boldsymbol{a},\boldsymbol{b}|} = \big|\measuredangle(\boldsymbol{a},\boldsymbol{b})\big|$ and $\vartheta^{[\hat{\boldsymbol{\omega}}]}_{|\boldsymbol{a},\boldsymbol{b}|} = \vartheta^{[\hat{\boldsymbol{\omega}}]}_{|\boldsymbol{b},\boldsymbol{a}|} = \big|\measuredangle_{\hat{\boldsymbol{\omega}}}(\boldsymbol{a},\boldsymbol{b})\big|$ are introduced.

For arbitrary $[\hat{\boldsymbol{\omega}}]$, the inequality $\vartheta^{[\hat{\boldsymbol{\omega}}]}_{|\boldsymbol{a},\boldsymbol{b}|} \geq \vartheta_{|\boldsymbol{a},\boldsymbol{b}|}$ holds. In case of $\boldsymbol{a} \in \hat{\boldsymbol{\omega}}^{\perp}$ and $\boldsymbol{b} \in \hat{\boldsymbol{\omega}}^{\perp}$, this is fulfilled with equality, and the two definitions correspond. For a reflected vector $\boldsymbol{b}$, the angle $\vartheta^{[\hat{\boldsymbol{\omega}}]}_{|\boldsymbol{a},-\boldsymbol{b}|}$ is the *supplementary* angle of $\vartheta^{[\hat{\boldsymbol{\omega}}]}_{|\boldsymbol{a},\boldsymbol{b}|}$ as $\vartheta^{[\hat{\boldsymbol{\omega}}]}_{|\boldsymbol{a},-\boldsymbol{b}|} = \pi - \vartheta^{[\hat{\boldsymbol{\omega}}]}_{|\boldsymbol{a},\boldsymbol{b}|}$.

Undirected Angles for Lines. Given two lines $[\boldsymbol{a}]$ and $[\boldsymbol{b}]$ instead of vectors $\boldsymbol{a}$ and $\boldsymbol{b}$, a direction of the angle between these is not meaningful. However, two different angles can be distinguished as defined next. See also Figure 1.

Definition 7 (Minimal and Maximal Angles)**.** Given two lines $[\boldsymbol{a}]$ and $[\boldsymbol{b}]$ the *minimal* (undirected) angle $\measuredangle([\boldsymbol{a}],[\boldsymbol{b}]) \in [0,\frac{\pi}{2}]$ and the the *maximal* (undirected) angle $\measuredangle^{[-1]}([\boldsymbol{a}],[\boldsymbol{b}]) \in [\frac{\pi}{2},\pi]$ between the lines $[\boldsymbol{a}]$ and $[\boldsymbol{b}]$ are defined as

$$\begin{aligned}\measuredangle\big([\boldsymbol{a}],[\boldsymbol{b}]\big) &:= \min\Big\{\,\vartheta_{|\boldsymbol{a},\boldsymbol{b}|}, \vartheta_{|\boldsymbol{a},-\boldsymbol{b}|}\,\Big\}\\ \measuredangle^{[-1]}\big([\boldsymbol{a}],[\boldsymbol{b}]\big) &:= \max\Big\{\,\vartheta_{|\boldsymbol{a},\boldsymbol{b}|}, \vartheta_{|\boldsymbol{a},-\boldsymbol{b}|}\,\Big\}\,.\end{aligned}$$

Given three lines $[\boldsymbol{a}]$, $[\boldsymbol{b}]$, and $[\hat{\boldsymbol{\omega}}]$, the *minimal* (undirected) angle $\measuredangle_{[\hat{\boldsymbol{\omega}}]}([\boldsymbol{a}],[\boldsymbol{b}]) \in [0,\frac{\pi}{2}]$ and the the *maximal* (undirected) angle $\measuredangle^{[-1]}_{[\hat{\boldsymbol{\omega}}]}([\boldsymbol{a}],[\boldsymbol{b}]) \in [\frac{\pi}{2},\pi]$ between the lines $[\boldsymbol{a}]$ and $[\boldsymbol{b}]$ measured with respect to $[\hat{\boldsymbol{\omega}}]$ are defined as

$$\begin{aligned}\measuredangle_{[\hat{\boldsymbol{\omega}}]}\big([\boldsymbol{a}],[\boldsymbol{b}]\big) &:= \min\Big\{\,\vartheta^{[\hat{\boldsymbol{\omega}}]}_{|\boldsymbol{a},\boldsymbol{b}|}, \vartheta^{[\hat{\boldsymbol{\omega}}]}_{|\boldsymbol{a},-\boldsymbol{b}|}\,\Big\}\\ \measuredangle^{[-1]}_{[\hat{\boldsymbol{\omega}}]}\big([\boldsymbol{a}],[\boldsymbol{b}]\big) &:= \max\Big\{\,\vartheta^{[\hat{\boldsymbol{\omega}}]}_{|\boldsymbol{a},\boldsymbol{b}|}, \vartheta^{[\hat{\boldsymbol{\omega}}]}_{|\boldsymbol{a},-\boldsymbol{b}|}\,\Big\}\,.\end{aligned}$$

As abbrevations, the notations $\vartheta_{[\boldsymbol{a}|\boldsymbol{b}]} = \measuredangle\big([\boldsymbol{a}],[\boldsymbol{b}]\big)$ and $\vartheta_{]\boldsymbol{a}|\boldsymbol{b}[} = \measuredangle^{[-1]}\big([\boldsymbol{a}],[\boldsymbol{b}]\big)$ as well as $\vartheta^{[\hat{\boldsymbol{\omega}}]}_{[\boldsymbol{a}|\boldsymbol{b}]} = \measuredangle_{[\hat{\boldsymbol{\omega}}]}\big([\boldsymbol{a}],[\boldsymbol{b}]\big)$ and $\vartheta^{[\hat{\boldsymbol{\omega}}]}_{]\boldsymbol{a}|\boldsymbol{b}[} = \measuredangle^{[-1]}_{[\hat{\boldsymbol{\omega}}]}\big([\boldsymbol{a}],[\boldsymbol{b}]\big)$ are introduced.

As before, the two definitions correspond in the case that $\boldsymbol{a} \in \hat{\boldsymbol{\omega}}^{\perp}$ and $\boldsymbol{b} \in \hat{\boldsymbol{\omega}}^{\perp}$ and the superindex can be omitted. Minimal and maximal angles are supplements of π to each other; for example, $\vartheta^{[\hat{\boldsymbol{\omega}}]}_{]\boldsymbol{a}|\boldsymbol{b}[}$ is the *supplementary* angle of $\vartheta^{[\hat{\boldsymbol{\omega}}]}_{[\boldsymbol{a}|\boldsymbol{b}]}$ with $\vartheta^{[\hat{\boldsymbol{\omega}}]}_{]\boldsymbol{a}|\boldsymbol{b}[} = \pi - \vartheta^{[\hat{\boldsymbol{\omega}}]}_{[\boldsymbol{a}|\boldsymbol{b}]}$.

---

[6] Obtained from the identities $\boldsymbol{a} * \boldsymbol{b} = \cos|\measuredangle(\boldsymbol{a},\boldsymbol{b})| \cdot \|\boldsymbol{a}\| \cdot \|\boldsymbol{b}\|$ and $\|\boldsymbol{a} \times \boldsymbol{b}\| = \sin|\measuredangle(\boldsymbol{a},\boldsymbol{b})| \cdot \|\boldsymbol{a}\| \cdot \|\boldsymbol{b}\|$.

[7] Numerically, the defintion via atan_2 is preferable, see [22].

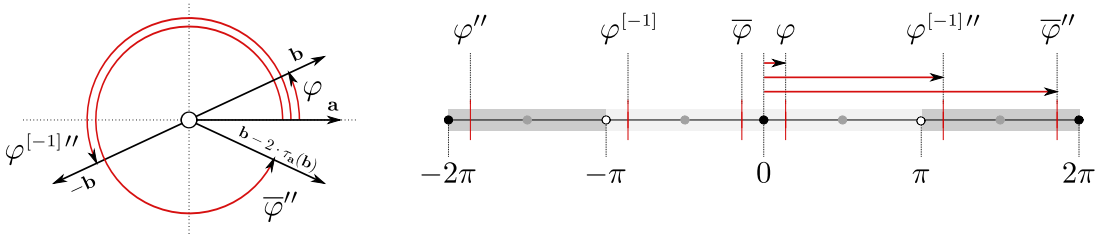

FIGURE 12. Example of a directed angle $\varphi = +\frac{25^\circ}{360^\circ} \cdot 2\pi \in (-\pi, \pi]$ from $\boldsymbol{a}$ to $\boldsymbol{b}$, together with the related inverted and the conjugated angle, and their dual values.

Directed Angles for Vectors. The *directed angle* $\measuredangle(\boldsymbol{a}, \boldsymbol{b}) \in (-\pi, \pi]$ 'from $\boldsymbol{a}$ to $\boldsymbol{b}$' is only defined if the plane $\operatorname{span}(\boldsymbol{a}, \boldsymbol{b})$ is equipped with an *orientation*, given by a third, fixed vector $\boldsymbol{n}$, perpendicular to $\operatorname{span}(\boldsymbol{a}, \boldsymbol{b})$. Vector $\boldsymbol{n}$ directs towards the 'point of view' onto the plane $\operatorname{span}(\boldsymbol{a}, \boldsymbol{b})$. For example, if the vectors $\boldsymbol{a}$ and $\boldsymbol{b}$ lie in the xy-plane $\boldsymbol{n}$ is typically set to $\boldsymbol{e}_z$. As for the definitions above, a generalization is defined for the case that $\boldsymbol{n}$ is substituted by a non-orthogonal vector $\hat{\boldsymbol{\omega}}$. Before the formal Definition 10, two tools are introduced.

Definition 8 (Atan$_2^\star$ Function)**.** For $x, y \in \mathbb{R}$, the bivariate function $\operatorname{atan}_2^\star : \mathbb{R} \times \mathbb{R} \to (-\pi, \pi]$ is defined as

$$\operatorname{atan}_2^\star(y, x) = \begin{cases} \operatorname{atan}\frac{y}{x} & x > 0 \\ \operatorname{atan}\frac{y}{x} + \operatorname{sign}^\star(y) \cdot \pi & x < 0 \\ \operatorname{sgn}(y) \cdot \frac{\pi}{2} & x = 0 \end{cases} .$$

The notation $\operatorname{atan}_2^\star \frac{y}{x} = \operatorname{atan}_2^\star(y, x)$ is introduced to maintain the fractional relation of the arguments y and x.

Definition 9 (Sign* and Acos$_2^\star$ Function)**.** For $x, y \in \mathbb{R}$, the generalized sign function $\operatorname{sign}^\star : \mathbb{R} \to \{-1, +1\}$ and the bivariate function $\operatorname{acos}_2^\star : \mathbb{R} \times \mathbb{R} \to (-\pi, \pi]$ are defined as

$$\operatorname{sign}^\star(x) := \begin{cases} +1 & x \geq 0 \\ -1 & x < 0 \end{cases}$$
$$\operatorname{acos}_2^\star(x, y) := \operatorname{sign}^\star(x) \cdot \operatorname{acos}(y) .$$

The inverse cosine function 'acos$_2^\star$' corresponds to the inverse tangent function 'atan$_2^\star$', see Figure 13 and Figure 14 for visualizations.

The function 'atan$_2^\star$' allows an inversion for a directed angle $\varphi \in (-\pi, \pi]$ since $\operatorname{atan}_2^\star \frac{\sin(\varphi)}{\cos(\varphi)} = \varphi$ holds. In more detail, for $\varphi \in (-\pi, \pi]$ it holds

$$\begin{aligned} \operatorname{atan}_2^\star \frac{\sin(\varphi)}{\cos(\varphi)} &= \operatorname{atan}_2^\star \frac{\operatorname{sgn}(\varphi) \cdot \sin|\varphi|}{\cos|\varphi|} \\ &= \operatorname{sgn}(\varphi) \cdot \operatorname{atan}_2^\star \frac{\sin|\varphi|}{\cos|\varphi|} = \operatorname{sgn}(\varphi) \cdot |\varphi| = \varphi . \end{aligned} \tag{A.1}$$

In the same manner, the bivariate, inverse cosine function 'acos$_2^\star$' allows an inversion for a directed angle $\varphi \in (-\pi, \pi]$ since the equations

$$\operatorname{acos}_2\big(\sin(\varphi), \cos(\varphi)\big) = \operatorname{sgn}(\varphi) \cdot \operatorname{acos}\big(\cos(\varphi)\big) = \operatorname{sgn}(\varphi) \cdot |\varphi| = \varphi \tag{A.2}$$

hold. In case of undirected angles, $|\varphi| \in [0, \pi]$, Equations A.1 and A.2 simplify to

$$\operatorname{atan}_2^\star \frac{\sin(|\varphi|)}{\cos(|\varphi|)} = \operatorname{acos}_2\big(|\sin(\varphi)|, \cos(\varphi)\big) = \operatorname{acos}\big(\cos(\varphi)\big) = |\varphi| . \tag{A.3}$$

In particular, for $c = \cos(\varphi)$, with $0 \leq c \leq 1$, it is $\sqrt{1 - c^2} = |\sin(\varphi)| = \sin(|\varphi|)$ such that the previous equations simplify to

$$\operatorname{atan}_2^\star \frac{\sqrt{1 - c^2}}{c} = \operatorname{atan}_2^\star \frac{|\sin(\varphi)|}{\cos(\varphi)} = \operatorname{acos}(c) = |\varphi| . \tag{A.4}$$

		Absolute		Relative		
Axis	**Term**	**Symbol**	**Example**	**Symbol**	**Example**	**Interval**
Vectors	Directed	$\measuredangle_{\boldsymbol{n}}(\boldsymbol{a},\boldsymbol{b})$	$\vartheta^{\langle \boldsymbol{n}\rangle}_{(\boldsymbol{b},\boldsymbol{a})} = \overline{\vartheta}^{\langle \boldsymbol{n}\rangle}_{(\boldsymbol{a},\boldsymbol{b})}$	$\measuredangle_{\hat{\boldsymbol{\omega}}}(\boldsymbol{a},\boldsymbol{b})$	$\vartheta^{\langle \hat{\boldsymbol{\omega}}\rangle}_{(\boldsymbol{b},\boldsymbol{a})} = \overline{\vartheta}^{\langle \hat{\boldsymbol{\omega}}\rangle}_{(\boldsymbol{a},\boldsymbol{b})}$	$(-\pi,\pi]$
	Inverse	$\measuredangle^{[-1]}_{\boldsymbol{n}}(\boldsymbol{a},\boldsymbol{b})$	$\vartheta^{\langle \boldsymbol{n}\rangle}_{(-\boldsymbol{b},\boldsymbol{a})} = \overline{\vartheta}^{\langle \boldsymbol{n}\rangle}_{(\boldsymbol{a},-\boldsymbol{b})}$	$\measuredangle^{[-1]}_{\hat{\boldsymbol{\omega}}}(\boldsymbol{a},\boldsymbol{b})$	$\vartheta^{\langle \hat{\boldsymbol{\omega}}\rangle}_{(-\boldsymbol{b},\boldsymbol{a})} = \overline{\vartheta}^{\langle \hat{\boldsymbol{\omega}}\rangle}_{(\boldsymbol{a},-\boldsymbol{b})}$	$(-\pi,\pi]$
	Undirected	$\big\lvert\measuredangle(\boldsymbol{a},\boldsymbol{b})\big\rvert$	$\vartheta_{\lvert \boldsymbol{a},\boldsymbol{b}\rvert} = \vartheta_{\lvert \boldsymbol{b},\boldsymbol{a}\rvert}$	$\big\lvert\measuredangle_{[\hat{\boldsymbol{\omega}}]}(\boldsymbol{a},\boldsymbol{b})\big\rvert$	$\vartheta^{[\hat{\boldsymbol{\omega}}]}_{\lvert \boldsymbol{a},\boldsymbol{b}\rvert} = \vartheta^{[\hat{\boldsymbol{\omega}}]}_{\lvert \boldsymbol{b},\boldsymbol{a}\rvert}$	$[0,\pi]$
Lines	Minimal	$\measuredangle\big([\boldsymbol{a}],[\boldsymbol{b}]\big)$	$\vartheta_{[\boldsymbol{a}\lvert\boldsymbol{b}]} = \vartheta_{[\boldsymbol{b}\lvert\boldsymbol{a}]}$	$\measuredangle_{[\hat{\boldsymbol{\omega}}]}\big([\boldsymbol{a}],[\boldsymbol{b}]\big)$	$\vartheta^{[\hat{\boldsymbol{\omega}}]}_{[\boldsymbol{a}\lvert\boldsymbol{b}]} = \vartheta^{[\hat{\boldsymbol{\omega}}]}_{[\boldsymbol{b}\lvert\boldsymbol{a}]}$	$[0,\pi/2]$
	Maximal	$\measuredangle^{[-1]}\big([\boldsymbol{a}],[\boldsymbol{b}]\big)$	$\vartheta_{]\boldsymbol{a}\lvert\boldsymbol{b}[} = \vartheta_{]\boldsymbol{b}\lvert\boldsymbol{a}[}$	$\measuredangle^{[-1]}_{[\hat{\boldsymbol{\omega}}]}\big([\boldsymbol{a}],[\boldsymbol{b}]\big)$	$\vartheta^{[\hat{\boldsymbol{\omega}}]}_{]\boldsymbol{a}\lvert\boldsymbol{b}[} = \vartheta^{[\hat{\boldsymbol{\omega}}]}_{]\boldsymbol{b}\lvert\boldsymbol{a}[}$	$[\pi/2,\pi]$

TABLE 4. Overview of notations for absolute and relative angles for (directed) vectors and (undirected) lines.

Before defining directed angles between vectors, it is needed that the *orientation* of three vectors can be computed as

$$\operatorname{ornt}^{\star}_3(\boldsymbol{a},\boldsymbol{b},\boldsymbol{c}) = \operatorname{sign}^{\star}\big(\det(\boldsymbol{a}\,\boldsymbol{b}\,\boldsymbol{c})\big)\,.$$

Alternately, '$\operatorname{ornt}^{\star}_3$' can be expressed via a scalar triple product as $\operatorname{ornt}^{\star}_3(\boldsymbol{a},\boldsymbol{b},\hat{\boldsymbol{\omega}}) = \operatorname{sign}^{\star}((\boldsymbol{a}\times\boldsymbol{b})*\hat{\boldsymbol{\omega}})$; for a planar illustration, see Figure 15. (Using '$\operatorname{sign}^{\star}$' instead of 'sgn' is useful in cases when $\vartheta_{[\boldsymbol{a}\lvert\boldsymbol{b}]} = \pi$.)

Definition 10 (Directed Angles and $\operatorname{Acos}^{\star}_3$ Function)**.** Given a vector $\boldsymbol{n}$ and two vectors $\boldsymbol{a}$ and $\boldsymbol{b}$ in $\boldsymbol{n}^{\perp}$, the (absolute) *directed* angle $\measuredangle_{\boldsymbol{n}}(\boldsymbol{a},\boldsymbol{b}) \in (-\pi,\pi]$ between $\boldsymbol{a}$ and $\boldsymbol{b}$ is defined as

$$\begin{aligned}\measuredangle_{\boldsymbol{n}}(\boldsymbol{a},\boldsymbol{b}) &= \operatorname{acos}^{\star}_2\big(\det(\boldsymbol{a}\,\boldsymbol{b}\,\boldsymbol{n}), \hat{\boldsymbol{a}}*\hat{\boldsymbol{b}}\big)\\ &= \operatorname{ornt}^{\star}_3(\boldsymbol{a},\boldsymbol{b},\boldsymbol{n})\cdot\operatorname{acos}(\hat{\boldsymbol{a}}*\hat{\boldsymbol{b}})\,.\end{aligned}$$

The *relative directed* angle between $\boldsymbol{a}$ and $\boldsymbol{b}$ measured with respect to a (directed) axis $\hat{\boldsymbol{\omega}}$ is denoted as $\measuredangle_{\hat{\boldsymbol{\omega}}}(\boldsymbol{a},\boldsymbol{b}) \in (-\pi,\pi]$ and defined via the trivariate function $\operatorname{acos}^{\star}_3 : \mathbb{R}^3\times\mathbb{R}^3\times\mathcal{S}^2 \to (-\pi,\pi]$ as

$$\begin{aligned}\measuredangle_{\hat{\boldsymbol{\omega}}}(\boldsymbol{a},\boldsymbol{b}) &= \operatorname{acos}^{\star}_3(\boldsymbol{a},\boldsymbol{b};\hat{\boldsymbol{\omega}})\\ &= \operatorname{acos}_2\big(\det(\boldsymbol{a}\,\boldsymbol{b}\,\hat{\boldsymbol{\omega}}), \hat{\tau}_{\hat{\boldsymbol{\omega}}}(\boldsymbol{a})*\hat{\tau}_{\hat{\boldsymbol{\omega}}}(\boldsymbol{b})\big)\\ &= \operatorname{ornt}^{\star}_3(\boldsymbol{a},\boldsymbol{b},\hat{\boldsymbol{\omega}})\cdot\operatorname{acos}\big(\hat{\tau}_{\hat{\boldsymbol{\omega}}}(\boldsymbol{a})*\hat{\tau}_{\hat{\boldsymbol{\omega}}}(\boldsymbol{b})\big)\,.\end{aligned} \tag{A.5}$$

As abbrevations, the terms $\vartheta^{\langle\hat{\boldsymbol{\omega}}\rangle}_{(\boldsymbol{b},\boldsymbol{a})} = \vartheta^{\langle-\hat{\boldsymbol{\omega}}\rangle}_{(\boldsymbol{a},\boldsymbol{b})} = \measuredangle_{\hat{\boldsymbol{\omega}}}(\boldsymbol{a},\boldsymbol{b})$ and $\overline{\vartheta}^{\langle\hat{\boldsymbol{\omega}}\rangle}_{(\boldsymbol{a},\boldsymbol{b})} = \vartheta^{\langle-\hat{\boldsymbol{\omega}}\rangle}_{(\boldsymbol{a},\boldsymbol{b})} = \measuredangle_{\hat{\boldsymbol{\omega}}}(\boldsymbol{a},\boldsymbol{b})$ are introduced.

As before, in the case that $\boldsymbol{a} \in \hat{\boldsymbol{\omega}}^{\perp}$ and $\boldsymbol{b} \in \hat{\boldsymbol{\omega}}^{\perp}$, the two definitions coincide. For dealing with directed angles along a mirrored perpendicular, $(-1)\cdot\boldsymbol{n}$, or between mirrored vectors ($-\boldsymbol{a}$ or $-\boldsymbol{b}$), two related concepts are introduced.

Definition 11 (Conjugation and Inversion)**.** Let φ be a directed angle in $(-\pi,\pi]$ define (i) the *conjugate* angle $\overline{\varphi} \in (-\pi,\pi]$, and (ii) the *inverse* angle $\varphi^{[-1]} \in (-\pi,\pi]$ as

$$\overline{\varphi} := -\varphi + \delta_{\pi}(\varphi)\cdot 2\pi \qquad\qquad \varphi^{[-1]} := \varphi + \operatorname{sign}^{\star}(-\varphi)\cdot\pi\,,$$

where the delta function $\delta = \delta_y(x) = \delta(x;y)$ is defined as $\delta(x;y) = \begin{cases} 1 & x = y \\ 0 & x \neq y \end{cases}$.

The *conjugation* corresponds to a 'reflection at 0', the conjugate angle $\overline{\varphi}$ is the 'signed variant' of the *explementary* angle $\varphi^{\overline{2\pi}} := 2\pi - \varphi \cong 0 - \varphi$. The *inversion* corresponds to a 'reflection at π', the inverse angle $\phi^{[-1]}$ is the 'signed variant' of the *complementary* angle $\varphi^{\overline{\pi}} := \pi - \varphi$. An overview of the concepts of the Definitions 6, 7, 10 and 11 is given within Table 4; in Figure 12 an example is illustrated.

Active and Passive. The introduced abbrevations for (directed) angles allow the *active* and the *passive interpretation* of angles as

$$\begin{aligned}\measuredangle_{\hat{\boldsymbol{\omega}}}(\boldsymbol{a},\boldsymbol{b}) = \operatorname{acos}^{\star}_3(\boldsymbol{a},\boldsymbol{b};\hat{\boldsymbol{\omega}}) &= \vartheta^{(\boldsymbol{b},\boldsymbol{a})}_{\langle\hat{\boldsymbol{\omega}}\rangle}\\ = \vartheta^{(\boldsymbol{a},\boldsymbol{b})}_{\langle-\hat{\boldsymbol{\omega}}\rangle} = \overline{\vartheta}^{(\boldsymbol{a},\boldsymbol{b})}_{\langle\hat{\boldsymbol{\omega}}\rangle} &= \overline{\vartheta}^{\langle\hat{\boldsymbol{\omega}}\rangle}_{(\boldsymbol{a},\boldsymbol{b})} = \vartheta^{\langle-\hat{\boldsymbol{\omega}}\rangle}_{(\boldsymbol{a},\boldsymbol{b})} = \vartheta^{\langle\hat{\boldsymbol{\omega}}\rangle}_{(\boldsymbol{b},\boldsymbol{a})}\,.\end{aligned}$$

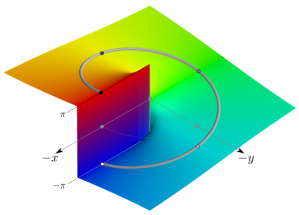

FIGURE 13. Plot of the function $\operatorname{atan}_2^\star(y,x)$ with emphasized image of the circle $(x,y)=(\cos(\varphi),\sin(\varphi))$ for $\varphi\in(-\pi,\pi]$.

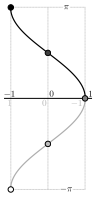

FIGURE 14. Two branches of $\operatorname{acos}_2^\star(y,x)$ with inverted x axes.

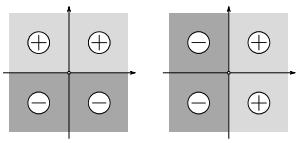

FIGURE 15. Sketches of $\operatorname{ornt}_2(\boldsymbol{a},\boldsymbol{b})=\operatorname{sign}^\star(\det(\boldsymbol{a}\;\boldsymbol{b}))$ and of $\operatorname{sgn}(\boldsymbol{a}*\boldsymbol{b})$ with $\boldsymbol{a}=(0,1)^T$.

Verbally, the *directed angle* $\measuredangle(\boldsymbol{a},\boldsymbol{b};\hat{\boldsymbol{\omega}})$ around $\hat{\boldsymbol{\omega}}$ which 'actively' maps $\boldsymbol{a}$ to $\boldsymbol{b}$ is denoted with *right-to-left* arguments in the superscript of $\vartheta_{\langle\hat{\boldsymbol{\omega}}\rangle}^{(\boldsymbol{b},\boldsymbol{a})}$. It equals the *directed angle* around $\hat{\boldsymbol{\omega}}$ which 'passively' maps $\boldsymbol{b}$ to $\boldsymbol{a}$, this is denoted with *left-to-right* arguments in the subscript of $\vartheta_{\langle\boldsymbol{b},\boldsymbol{a}\rangle}^{\langle\hat{\boldsymbol{\omega}}\rangle}$.

APPENDIX B. VECTORIAL AND ANGLE AXIS REPRESENTATION

Here, the Lie algebra $so(3)$ of skew-symmetric (3×3) matrices is briefly called *tangential space*. An element $\phi\cdot\hat{\boldsymbol{\omega}}^\otimes$ of $so(3)$ is briefly called *tangential vector*. Given a rotation matrix $\boldsymbol{R}\in SO(3)$, the corresponding tangential vector $\phi\cdot\hat{\boldsymbol{\omega}}^\otimes\in so(3)$ is computed via the logarithmic map as

$$\phi\cdot\hat{\boldsymbol{\omega}}^\otimes=\ln(\boldsymbol{R})=\frac{\phi}{2\cdot\sin\phi}\cdot(\boldsymbol{R}-\boldsymbol{R}^T)\,. \tag{B.1}$$

In the other direction, given a tangential vector $\phi\cdot\hat{\boldsymbol{\omega}}^\otimes\in so(3)$, the corresponding rotation matrix $\boldsymbol{R}=\exp(\phi\cdot\hat{\boldsymbol{\omega}}^\otimes)\in SO(3)$ is determined via the exponential map (*Rodrigues formula*) as

$$\boldsymbol{R}=\boldsymbol{I}+\sin\phi\cdot\hat{\boldsymbol{\omega}}^\otimes+(1-\cos\phi)\cdot(\hat{\boldsymbol{\omega}}^\otimes)^2\,. \tag{B.2}$$

Fixated Rotation Axis. For deriving a tuple of *angle* and *axis* $(\phi,\hat{\boldsymbol{\omega}})$ from a tangential vector $\phi\cdot\hat{\boldsymbol{\omega}}$, *two* options are described: The first option is to constrain the rotation angle, such that $\phi\in[0,\pi]$ holds: in this case, the sign information is contained in the 'changing' orientation of the axis $\hat{\boldsymbol{\omega}}$. The second option is to allow $\phi\in(-\pi,\pi]$ and to fixate the orientation of the rotation axis (to a given physical setup), such that for all rotations about a line $[\hat{\boldsymbol{\omega}}]$, it is ensured that the same representative $\hat{\boldsymbol{\omega}}$ is used. For example, these two options were crucial in the proof of the mutual orthogonality of toroids $\mathcal{T}^{[+]}$ and $\mathcal{T}^{[-]}$ in Section 3.2. For a given rotation matrix $\boldsymbol{R}$, the first option with $\phi\in[0,\pi]$ is computed using the direct formulas given in the next definition.

Definition 12 (Hashed Angle and Axis)**.** Given rotation matrix $\boldsymbol{R}\in SO(3)$, (i) the hashed (undirected) angle $\phi_{\boldsymbol{R}}^\#\in[0,\pi]$, and (ii) the hashed (directed) rotation axis $\boldsymbol{\omega}_{\boldsymbol{R}}^\#\in\mathcal{S}^2$ are defined as

$$\begin{aligned}\phi_{\boldsymbol{R}}^\#&=\operatorname{ang}^\#(\boldsymbol{R}):=\operatorname{acos}\Big(\frac{\operatorname{tr}(\boldsymbol{R})-1}{2}\Big)\\ \boldsymbol{\omega}_{\boldsymbol{R}}^\#&=\operatorname{ax}^\#(\boldsymbol{R}):=(\boldsymbol{R}-\boldsymbol{R}^T)^\oplus\,.\end{aligned}$$

Given a rotation matrix $\boldsymbol{R}$ and a *fixed* axis $\hat{\boldsymbol{\omega}}$ the *sign* of the hashed angle $\phi_{\boldsymbol{R}}^\#$ and the hashed axis $\boldsymbol{\omega}_{\boldsymbol{R}}^\#$ can be 'corrected' to the second option via the next definition.

Definition 13 (Argument of a Rotation)**.** Given a rotation matrix $\boldsymbol{R}\in SO(3)$ and a fixed, oriented axis $\hat{\boldsymbol{\omega}}\in\mathcal{S}^2$, the rotation argument 'directed angle' $\phi=\arg(\boldsymbol{R},\hat{\boldsymbol{\omega}})\in(-\pi,\pi]$ is computed as

$$\phi=\arg(\boldsymbol{R},\hat{\boldsymbol{\omega}}):=\operatorname{acos}_2\big(\hat{\boldsymbol{\omega}}*(\boldsymbol{R}-\boldsymbol{R}^T)^\oplus,\tfrac{\operatorname{tr}(\boldsymbol{R})-1}{2}\big)=\operatorname{sgn}(\hat{\boldsymbol{\omega}}*\boldsymbol{\omega}_{\boldsymbol{R}}^\#)\cdot\phi_{\boldsymbol{R}}^\#\,. \tag{B.3}$$

The issue of computing the *sign* of an angle ϕ (resp. the orientation of an axis $\hat{\boldsymbol{\omega}}$) appears several times in this text. In particular, Equation A.1 and Equation A.2 are of the form $\phi=\operatorname{sgn}(\phi)\cdot|\phi|$. This form also appears in Equation A.5 and Equation B.3 and is important in the final Section C.

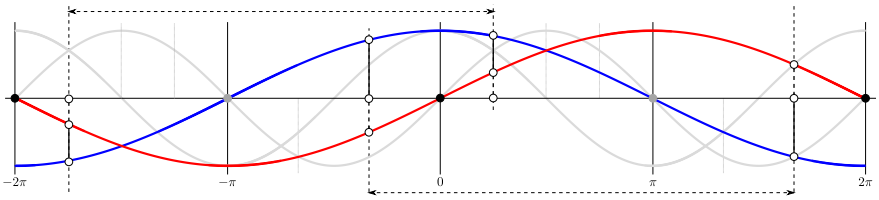

FIGURE 16. Functions $\sin(\frac{\phi}{2})$ and $\cos(\frac{\phi}{2})$ (in red and blue) with angles, $\frac{1}{4}\pi \cong -\frac{7}{4}\pi$ and $\frac{5}{3}\pi \cong -\frac{1}{3}\pi$, with positive ($\phi^+$) and negative ($\phi^-$) values, or with principal (ϕ') and secondary (ϕ'') values.

Active and Passive. For rotation matrices, the active and the passive interpretations are the following: An active rotation $\boldsymbol{R}_{\mathsf{A}} : \boldsymbol{b} \xleftarrow{\mathsf{A}} \boldsymbol{a}$ with $\boldsymbol{R}_{\mathsf{A}} \equiv \boldsymbol{R}(\vartheta^{(\boldsymbol{b},\boldsymbol{a})}, \hat{\boldsymbol{\omega}})$ is equivalent to $\boldsymbol{b} = \boldsymbol{R}(\vartheta^{(\boldsymbol{b},\boldsymbol{a})}_{\langle\hat{\boldsymbol{\omega}}\rangle}, \hat{\boldsymbol{\omega}}) \cdot \boldsymbol{a}$. This term is transposed to $\boldsymbol{b}^T = \boldsymbol{a} * \boldsymbol{R}^T(\vartheta^{(\boldsymbol{b},\boldsymbol{a})}_{\langle\hat{\boldsymbol{\omega}}\rangle}, \hat{\boldsymbol{\omega}}) = \boldsymbol{a} * \boldsymbol{R}(\vartheta^{(\boldsymbol{a},\boldsymbol{b})}_{\langle\hat{\boldsymbol{\omega}}\rangle}, \hat{\boldsymbol{\omega}})$ which is rewritten to $\boldsymbol{a} * \boldsymbol{R}(\vartheta^{\langle\hat{\boldsymbol{\omega}}\rangle}_{(\boldsymbol{a},\boldsymbol{b})}, \hat{\boldsymbol{\omega}}) = \boldsymbol{b}^T$. This is equivalent to the passive rotation $\boldsymbol{R}_{\mathsf{P}} : \boldsymbol{a} \xmapsto{\mathsf{P}} \boldsymbol{b}$ with $\boldsymbol{R}_{\mathsf{P}} \equiv \boldsymbol{R}(\vartheta^{\langle\hat{\boldsymbol{\omega}}\rangle}_{(\boldsymbol{a},\boldsymbol{b})}, \hat{\boldsymbol{\omega}})$, see also [4] for further details.

APPENDIX C. UNIT BALL AND QUATERNION REPRESENTATION

In this section, the relation between the *unit ball representation* (Definition 4) and the *unit quaternion representation* is described. The definition of a unit quaternion $\hat{q} \in \mathcal{S}^3$ in terms of angle and axis of a rotation reads as

$$\hat{q} = q_0 + \boldsymbol{i} * \boldsymbol{q} = \cos\frac{\phi}{2} + \sin\frac{\phi}{2} \cdot \boldsymbol{i} * \hat{\boldsymbol{\omega}} \,,$$

see for example, [4]. Generally, there are *two* quaternions that are identified with one rotation matrix $\boldsymbol{R}$, namely, $\hat{q}$ and $-\hat{q}$. As before (Section B), two ways are described which constrain the rotation angle so that one unique quaternion is obtained.

The first option is to require $\phi' \in (-\pi, \pi]$. This is equivalent to $\cos(\frac{\phi'}{2}) \geq 0$ (see Figure 16) and the unit quaternion $\hat{q}$ is element of the *'upper'* (with respect to $\boldsymbol{e}_z$) hemisphere of $\mathcal{S}^3$. The second option is to require $\phi^+ \in [0, 2\pi)$. This is equivalent to $\sin(\frac{\phi^+}{2}) \geq 0$ (see Figure 16) and the unit quaternion $\hat{q}$ is element of the *'upper'* (with respect to $\hat{\boldsymbol{\omega}}$) hemisphere of $\mathcal{S}^3$.

If the *first* angle convention is chosen, the *orientation* of rotation axis $\hat{\boldsymbol{\omega}}$ can not be determined from $\hat{q}$ (as in the formulas of Definition 12). If the *second* angle convention is chosen, it is possible to maintain the *orientation* of a *fixed* rotation axis $\hat{\boldsymbol{\omega}}$ within the quaternion $\hat{q}$ since a multiplication by $\sin(\frac{\phi^+}{2}) \geq 0$ for $\phi^+ \in [0, 2\pi)$ does not change the orientation.

In the case that the *second* option is chosen, such that $\phi^+ \in [0, 2\pi)$, the quaternion is emphasized by using a 'plus' as

$$\hat{q}^+ = (q_0^+, \boldsymbol{q}^+) = \big(\cos\big(\frac{\phi^+}{2}\big), \sin\big(\frac{\phi^+}{2}\big) \cdot \hat{\boldsymbol{\omega}}\big)$$

in vector notation. Then, the positive angle ϕ^+ and the fixed direction $\hat{\boldsymbol{\omega}}$ are computed as

$$\phi^+ = 2 \cdot \operatorname{acos}(q_0^+) \qquad\qquad \hat{\boldsymbol{\omega}} = (\boldsymbol{q}^+)^{\circledcirc} \,.$$

With this information, the primal and the dual rotation vectors of the unit ball representation, $\boldsymbol{v}'$ and $\boldsymbol{v}''$, are determined by $\phi' = \begin{cases} \phi^+ & \phi^+ \leq \pi \\ \phi^+ - 2\pi & \phi^+ > \pi \end{cases}$ and the equations in Defintions 3 and 4. As mentioned before, the quaternion reflected at the origin $\hat{q}^- := (-1) \cdot \hat{q}^+$ represents the same rotation $\boldsymbol{R}$ as the 'original' $\hat{q}^+$. In vector notation, $\hat{q}^-$ reads as

$$\hat{q}^- = (q_0^-, \boldsymbol{q}^-) = \big(\cos\big(\frac{\phi^-}{2}\big), \sin\big(\frac{\phi^-}{2}\big) \cdot \hat{\boldsymbol{\omega}}\big) \,.$$

Comparing $\hat{q}^+$ and $\hat{q}^-$, one observes that the reflection by '$\cdot(-1)$' sends the scalar part $q_0^+ = \cos(\frac{\phi^+}{2})$ to $q_0^- = -\cos(\frac{\phi^+}{2})$ and the factor $\sin(\frac{\phi^+}{2})$ of the vector part $\boldsymbol{q}^+$ to the factor $-\sin(\frac{\phi^+}{2})$ of $\boldsymbol{q}^-$. These two operations correspond to the dualization of the primal angle ϕ^+ to the dual angle $(\phi^+)''$. For an illustration, see Figure 16.

In the case that the *first* convention $\phi' \in (-\pi, \pi]$ is chosen, this insight follows immediately. In both cases, the representation via a *unit quaternion* – following one of the two angle conventions – and the primal-dual *unit ball represention* of rotations are related by a bijection: the *reflection* at the origin of unit quaternions corresponds one-to-one to the 'shell-swaps' (*dualization*) inside the unit ball. Due to this correspondance, the unit ball representation may serve as an appropriate *visualization method* not only for rotations but also for unit quaternions.

Appendix D. Notation Overview

A notation overview about the symbols used in this document is given the within Table 5.

Symbol	**Example**	**Interpretation**
Operators		
'π'	$\pi_{\boldsymbol{a}}(\boldsymbol{b})$	*orthogonal projection* of $\boldsymbol{b}$ onto $\boldsymbol{a}$
'τ'	$\tau_{\boldsymbol{a}}(\boldsymbol{b})$	*orthogonal projection* of $\boldsymbol{b}$ into the orthogonal complement of $\boldsymbol{a}$
'$\cdot^{\circledcirc}$'	$\hat{\boldsymbol{a}} = \boldsymbol{a}^{\circledcirc}$	*normalized* version of $\boldsymbol{a}$ (scaled to length one)
'$\cdot^{\otimes}$'	$\boldsymbol{a}^{\otimes}$	*skew-symmetric matrix* to $\boldsymbol{a}$
'$\cdot^{\oplus}$'	$\boldsymbol{S}^{\oplus}$	*axis vector* to skew-symmetric matrix $\boldsymbol{S}$
'$*$'	$\boldsymbol{a} * \boldsymbol{b}$	*inner product* of $\boldsymbol{a}$ and $\boldsymbol{b}$
'$\cdot^{\boxtimes}$'	$\boldsymbol{a}^{\boxtimes}$	*'matrix-square'* of $\boldsymbol{a}$ / *outer product* of $\boldsymbol{a}$ and $\boldsymbol{a}$, $\boldsymbol{a}^{\boxtimes} = \boldsymbol{a} \cdot \boldsymbol{a}^T$
Angles		
'φ'		*unspecified* angle (assumed to be a primary angle)
	φ'	*primary value* of angle φ, in $(-\pi, \pi]$
	φ''	*secondary value* of angle φ, in $(-2\pi, 2\pi] \setminus (-\pi, \pi]$
	$\overline{\varphi}$	*conjugated* angle of φ (signed reflection at 0 / reflected axis)
	$\varphi^{[-1]}$	*inverted* angle of φ (signed reflection at π / one reflected vector)
Line Angles		
'ϑ'		angle *between* (directed) *vectors* or (undirected) *lines*
	$\vartheta^{\langle \hat{\boldsymbol{\omega}} \rangle}_{(\boldsymbol{b},\boldsymbol{a})}$	*(passive-)directed angle* from vector $\boldsymbol{a}$ to vector $\boldsymbol{b}$ along $\hat{\boldsymbol{\omega}}$
	$\vartheta^{[\hat{\boldsymbol{\omega}}]}_{\lvert \boldsymbol{a},\boldsymbol{b} \rvert}$	*undirected angle* between vectors $\boldsymbol{a}$ and $\boldsymbol{b}$ measured along line $[\hat{\boldsymbol{\omega}}]$
	$\vartheta^{[\hat{\boldsymbol{\omega}}]}_{[\boldsymbol{a}\rvert\boldsymbol{b}]}$	*minimal angle* between line $[\boldsymbol{a}]$ and line $[\boldsymbol{b}]$ along line $[\hat{\boldsymbol{\omega}}]$
	$\vartheta^{[\hat{\boldsymbol{\omega}}]}_{]\boldsymbol{a}\rvert\boldsymbol{b}[}$	*maximal angle* between line $[\boldsymbol{a}]$ and line $[\boldsymbol{b}]$ along line $[\hat{\boldsymbol{\omega}}]$
Rotations		
'ϕ'		argument of a *rotation*
	$\phi \cdot \hat{\boldsymbol{\omega}}$	*rotation vector* of angle ϕ and axis $\hat{\boldsymbol{\omega}}$
	$\phi \cdot \hat{\boldsymbol{\omega}}^{\otimes}$	*tangential vector* of angle ϕ and axis $\hat{\boldsymbol{\omega}}$
	$\boldsymbol{R}(\phi; \hat{\boldsymbol{\omega}})$	*rotation matrix* of angle ϕ and axis $\hat{\boldsymbol{\omega}}$, $\boldsymbol{R}(\phi; \hat{\boldsymbol{\omega}}) = \exp(\phi \cdot \hat{\boldsymbol{\omega}}^{\otimes})$
	$\hat{\boldsymbol{\omega}}^{\boxtimes} = \pi_{\hat{\boldsymbol{\omega}}}(\boldsymbol{R})$	*orthogonal projection* of $\boldsymbol{R}$ onto $\hat{\boldsymbol{\omega}}$, 'normal component' of $\boldsymbol{R}$
	$\boldsymbol{R}_{\Omega} = \tau_{\hat{\boldsymbol{\omega}}}(\boldsymbol{R})$	*orthogonal projection* of $\boldsymbol{R}$ onto $\Omega = \hat{\boldsymbol{\omega}}^{\perp}$, 'planar component' of $\boldsymbol{R}$
Functions		
'$\operatorname{atan}_2^{\star}$'	$\operatorname{atan}_2^{\star}(\sin\varphi, \cos\varphi)$	sign-consistent *inversion* of 'tan', as $\operatorname{atan}_2^{\star} \frac{\sin\varphi}{\cos\varphi} = \varphi$
'$\operatorname{acos}_2^{\star}$'	$\operatorname{acos}_2^{\star}(\sin\varphi, \cos\varphi)$	sign-consistent *inversion* of 'cos', as $\operatorname{acos}_2^{\star}(\sin\varphi, \cos\varphi) = \varphi$
'$\operatorname{sign}^{\star}$'	$\operatorname{sign}^{\star}(x)$	generalized *signum* func., as $\operatorname{sign}^{\star}(x) = \{+1 \text{ for } x \geq 0 \mid -1 \text{ for } x < 0\}$
'$\operatorname{ornt}_2^{\star}$'	$\operatorname{ornt}_2^{\star}(\boldsymbol{a}, \boldsymbol{b})$	*orientation* of the sorted set $(\boldsymbol{a}, \boldsymbol{b})$ of *two-dimensional* vectors
'$\operatorname{ornt}_3^{\star}$'	$\operatorname{ornt}_3^{\star}(\boldsymbol{a}, \boldsymbol{b}, \hat{\boldsymbol{\omega}})$	*orientation* of the sorted set $(\boldsymbol{a}, \boldsymbol{b}, \hat{\boldsymbol{\omega}})$ of *three-dimensional* vectors
'acos'	$\operatorname{acos}(\boldsymbol{a} * \boldsymbol{b})$	computation of the *absolute angle* between $\boldsymbol{a}$ and $\boldsymbol{b}$
'$\operatorname{acos}_3^{\star}$'	$\operatorname{acos}_3^{\star}(\boldsymbol{a}, \boldsymbol{b}; \hat{\boldsymbol{\omega}})$	comp. of the (active) *directed angle* from $\boldsymbol{a}$ to $\boldsymbol{b}$ measured along $\hat{\boldsymbol{\omega}}$

Table 5. Notation overview of operators, angles, rotations and functions.

References

[1] Alpern, B., Carter, L., Grayson, M., Pelkie, C.: Orientation maps: techniques for visualizing rotations (a consumer's guide). In: VIS '93: Proceedings of the 4th conference on Visualization '93, pp. 183–188 (1993)

[2] Bai, S., Angeles, J.: A unified input–output analysis of four-bar linkages. Mechanism and Machine Theory **43**(2), 240 – 251 (2008)

[3] Bauchau, O.A., Trainelli, L.: The vectorial parameterization of rotation. Nonlinear Dynamics **32**(1), 71–92 (2003)

[4] Bongardt, B.: Sheth-Uicker Convention Revisited – A Normal Form for Specifying Mechanisms. Tech. rep., RIC, DFKI, Bremen (2012)

[5] Davenport, P.B.: Rotations about nonorthogonal axes. AIAA Journal **11**(6), 853–857 (1973)

[6] Dorst, L., Fontijne, D., Mann, S.: Geometric Algebra – An Object-Oriented Approach to Geometry. Morgan Kaufmann Series in Computer Graphics. Morgan Kaufmann (2007)

[7] Freudenstein, F.: Approximate synthesis of four-bar linkages. Transaction ASME **77**, 853–861 (1955)

[8] Gupta, K.C.: Kinematic analysis of manipulators using the zero reference position description. International Journal of Robotics Research **5**, 5–13 (1986)

[9] Hanson, A.J.: Visualizing Quaternions. Morgan Kaufmann (2006)

[10] Hayes, M.J.D., Parsa, K., Angeles, J.: The effect of data-set cardinality on the design and structural errors of four-bar function-generators. In: 10th World Congress on the Theory of Machines and Mechanisms, pp. 437–442 (1999)

[11] Husty, M., Ottaviano, E., Ceccarelli, M.: A Geometrical Characterization of Workspace Singularities in 3R Manipulators. In: Advances in Robot Kinematics: Analysis and Design, pp. 411–418 (2008)

[12] Husty, M.L., Pfurner, M., Schröcker, H.P.: A new and efficient algorithm for the inverse kinematics of a general serial 6r manipulator. Mechanism and Machine Theory **42**(1), 66 – 81 (2007)

[13] Klein, F.: Elementary mathematics from an advanced standpoint: Arithmetic, Algebra, Analysis (1932)

[14] Kuipers, J.B.: Quaternions and Rotation Sequences: A Primer with Applications to Orbits, Aerospace and Virtual Reality. Princeton University Press (2002)

[15] Liu, Z., Angeles, J.: Least-square optimization of planar and spherical four-bar function generator under mobility constraints. Journal of Mechanical Design **114**(4), 569–573 (1992)

[16] Mladenova, C.D., Mladenov, I.M.: Vector decomposition of finite rotations. Reports on Mathematical Physics **68**(1), 107 – 117 (2011)

[17] Murray, R.M., Sastry, S.S., Zexiang, L.: A Mathematical Introduction to Robotic Manipulation. CRC Press, Boca Raton, FL, USA (1994)

[18] Paul, R.P., Stevenson, C.N.: Kinematics of robot wrists. International Journal of Robotics Research **2**, 31–38 (1983)

[19] Pfurner, M.: Analysis of spatial serial manipulators using kinematic mapping. Ph.D. thesis, University of Innsbruck, Austria (2006)

[20] Piovan, G., Bullo, F.: On coordinate-free rotation decomposition: Euler angles about arbitrary axes. IEEE Transactions on Robotics **28**(3), 728 –733 (2012)

[21] Selig, J.M.: Geometric Fundamentals of Robotics, 2nd ed. Springer, Berlin (2005)

[22] Shewchuk, J.R.: Lecture notes on geometric robustness (2009)

[23] Shuster, M.D., Markley, F.L.: Generalization of the euler angles. The Journal of the Astronautical Sciences **51**(2), 123–132 (2003)

[24] Stillwell, J.: Naive Lie Theory. Undergraduate Texts in Mathematics. Springer, New York, NY (2008)

[25] Yang, A.T., Freudenstein, F.: Application of dual-number quaternion algebra to the analysis of spatial mechanisms. Journal of Applied Mechanics **31**(2), 300–308 (1964)